Table 1. Details of the NoV outbreaks of gastroenteritis between 2002 and 2006 in Japan

Outbreak No.	Month and year	Area	Setting	Genogroup/genotype	Patients/persons at risk (attack rate)	Patients positive/tested	Food handlers			Food positive/tested
							total	symptomatic	asymptomatic	
							positive/tested	positive/tested	positive/tested	
1	Nov 02	Nagano	kindergarten	GII/2	50/124 (40)	3/3 (100)	1/5 (20)	1/1	0/4	NT
2	Nov 02	Nagano	caterer	GII/15	4/12 (33)	3/3 (100)	2/4 (50)	1/1	1/3	NT
3	Dec 02	Nagano	restaurant	GII/4	7/15 (47)	3/3 (100)	2/14 (14)	2/4	0/10	NT
4	Jan 03	Nagano	restaurant	GII/10	16/26 (62)	2/3 (67)	2/3 (67)	2/2	0/1	NT
5	Jan 03	Hokkaido	caterer	GII/3	27/63 (43)	9/9 (100)	2/4 (50)	0/0	2/4	NT
6	Mar 03	Kagoshima	school	GI/2	65/232 (28)	6/7 (86)	3/4 (75)	3/4	0/0	NT
7	Feb 04	Hokkaido	elderly care facility	GII/4	34/108 (31)	13/14 (93)	3/10 (30)	1/8	2/2	0/3
8	Mar 04	Gunma	bakery	GII 4	178/346 (51)	9/9 (100)	6/10 (60)	6/6	0/4	0/2
9	Jun 04	Gunma	restaurant	GII/2	112/3,611 (3)	6/6 (100)	12/28 (43)	unknown	unknown	0/1
10	Dec 04	Hokkaido	hotel	GII/4	68/250 (27)	11/12 (92)	2/5 (40)	0/0	2/5	NT
11	Dec 05	Gunma	restaurant	GII/7	43/281 (15)	6/6 (100)	4/6 (67)	unknown	unknown	NT
12	Mar 06	Gunma	hotel	GII/4	197/806 (24)	6/6 (100)	6/11 (55)	6/6	0/5	NT
Total					801/5,874 (14)	77/81 (95)	45/104 (43)			

NT = Not tested. Figures in parentheses are percentages.

A 10% (weight/volume) stool homogenate was prepared in phosphate-buffered saline (PBS). Food samples were prepared as described previously [13] using 10 g of food rinsed with 10 ml of PBS. Viral RNA was extracted from the stool specimens and food samples using the QIAamp Viral RNA Mini kit (Qiagen GmbH, Hilden, Germany). RNA solution was treated with 1 U of DNase I (Takara, Tokyo, Japan) for 30 min at 37°and then 30 μl of the solution was mixed with 20 μl of reverse transcription (RT) solution containing 100 mM Tris-HCl (pH 8.3), 150 mM KCl, 6 mM $MgCl_2$, 1 mM of dNTP mixture, 10 mM dithiothreitol, 75 pmol of random hexamer (Takara), 30 U of RNase inhibitor (Takara), and 200 U of reverse transcriptase [Superscript II, RNaseH (–); Invitrogen, San Diego, Calif., USA]. The mixture was incubated for 60 min at 42°and then for 15 min at 70°to inactivate the reverse transcriptase. The partial capsid region was amplified as previously described [14]. Briefly, for GI NoVs, COG1F and G1SKR primers were used for the 1st PCR and then G1SKF and G1SKR primers were used for the nested PCR. For GII NoVs, COG2F and G2SKR were used for the 1st PCR and then G2SKF and G2SKR primers were used for the nested PCR. The RT-PCR products were separated by 1.5% agarose gel electrophoresis excised from the gel and then purified using MinElute PCR Purification Kit (Qiagen). Real-time RT-PCR was performed in order to determine the viral loads as described previously [1]. The real-time PCR mixture contained 5 μl of cDNA (RT product), 17.5 μl of TaqMan Universal PCR Master Mix (Applied Biosystems, Foster City, Calif., USA), 400 nM of each primer, and fluorogenic probes (probes for GI, 10.5 pmol of RING1(a)-TP and 3.5 pmol of RING1(b)-TP; probe for GII, 3.5 pmol of RING2-TP). To quantitate copy numbers of the capsid gene of NoV, concentrations of the primers and probes have been optimized [1]. Nucleotide sequences were determined with an automated DNA sequencer (ABI 310 DNA sequencer, Applied Biosystems, Foster City, Calif., USA) using Dye Terminator Cycle Sequencing Ready Reaction Kit (Applied Biosystems). Nucleotide sequences were aligned with Clustal X (version 1.83.1), and the distances were calculated by Kimura's two-parameter method. Phylogenetic trees with bootstrap analysis from 1,000 replicas were generated by the neighbor-joining method, as described earlier [12]. Accession numbers for sequences determined in this study were AB427191–AB427202.

The attack rate (percentage of the number of patients/the number of persons at risk) varied between 3 and 62% (table 1). NoV was detected in 77 of 81 (95%) patients and 45 of 104 (43%) food handlers. At least 22 of 32 (63%) symptomatic food handlers were positive, and of 38 asymptomatic food handlers 7 (18%) were positive (the symptoms of 16 positive food handlers were unknown). At least one food handler from each outbreak was infect-

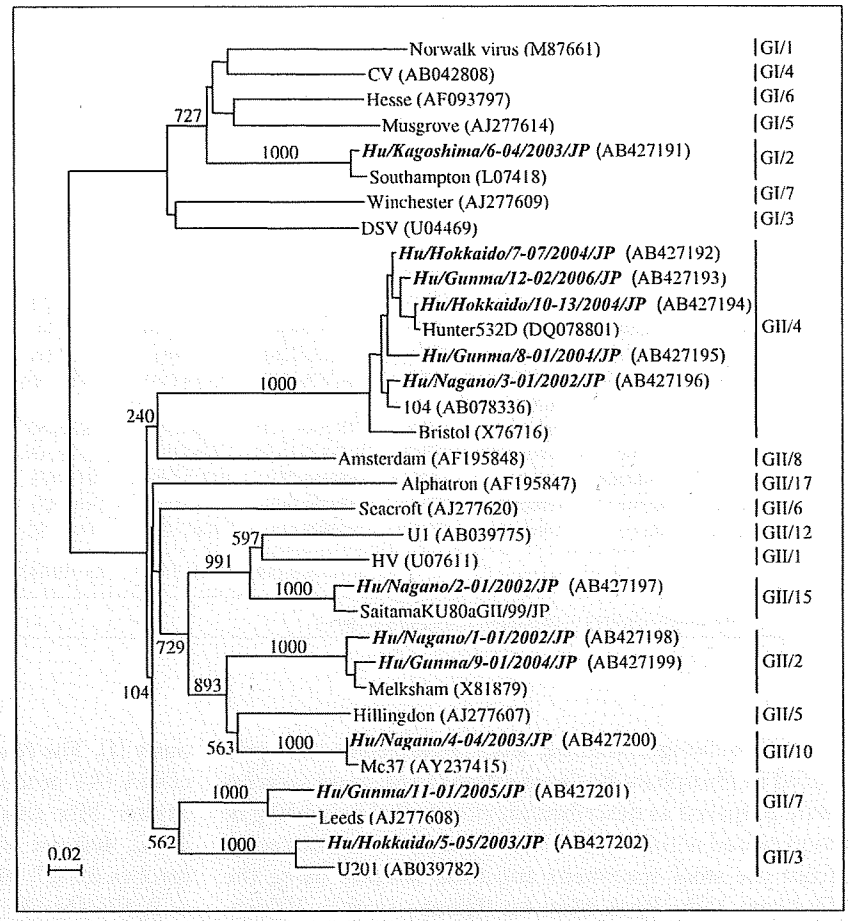

Fig. 1. Phylogenetic tree of the NoV nucleotide sequences detected in this study (represented in bold italics). NoV nucleotide sequences were constructed with the partial N-terminal capsid region [12]. Bootstrap values of 950 or higher were considered statistically significant for the grouping.

ed with NoV (table 1); however, the suspected contaminated food samples from 3 outbreaks were negative for NoV. Sequence analysis of the positive stool specimens was performed using the partial N-terminal capsid region. Seven different NoV genotypes were detected, GI/2, GII/2, GII/3, GII/4, GII/7, GII/10 and GII/15 (fig. 1). The majority of the outbreaks (4 of 12 outbreaks) were caused by GII/4 strains (table 1). The NoV nucleotide sequence detected in patients and food handlers were identical in each of the outbreaks, indicating that a single NoV strain was the cause of the outbreak.

The NoV viral loads in the stool specimens were measured by real-time RT-PCR (fig. 2). The viral load in patients ranged between 2.6×10^5 and 4.6×10^{12} copies/g stool with a mean viral load of 8.2×10^{10} copies/g stool. The viral load in symptomatic food handlers ranged between 3.9×10^6 and 7.7×10^{10} copies/g stool with a mean viral load of 4.5×10^9 copies/g stool. The viral load in the asymptomatic food handlers ranged between 4.7×10^7 and 1.3×10^9 copies/g of stool with a mean viral load of 6.7×10^8 and 7.2×10^6 copies/g of stool for GII/3 and GII/4, respectively (the means of the other genotypes could not be compared because the numbers were limited to one or not detected). In the present study, we assessed viral loads in stools collected from patients with NoV infection and food handlers. Recently, we found that asymptomatic NoV infections were widespread in the food catering industry in Japan [10]. More importantly, we found that the asymptomatic individuals had similar mean viral loads to the symptomatic individuals [10]. The current study has also shown that asymptomatic food handlers in Japan had high viral loads (between 4.7×10^7 and 1.3×10^9 copies/g of stool). Therefore, in order to control future NoV outbreaks, sanitary education and practices are essential for food handlers in order to reduce the spread of NoV in the food catering industries.

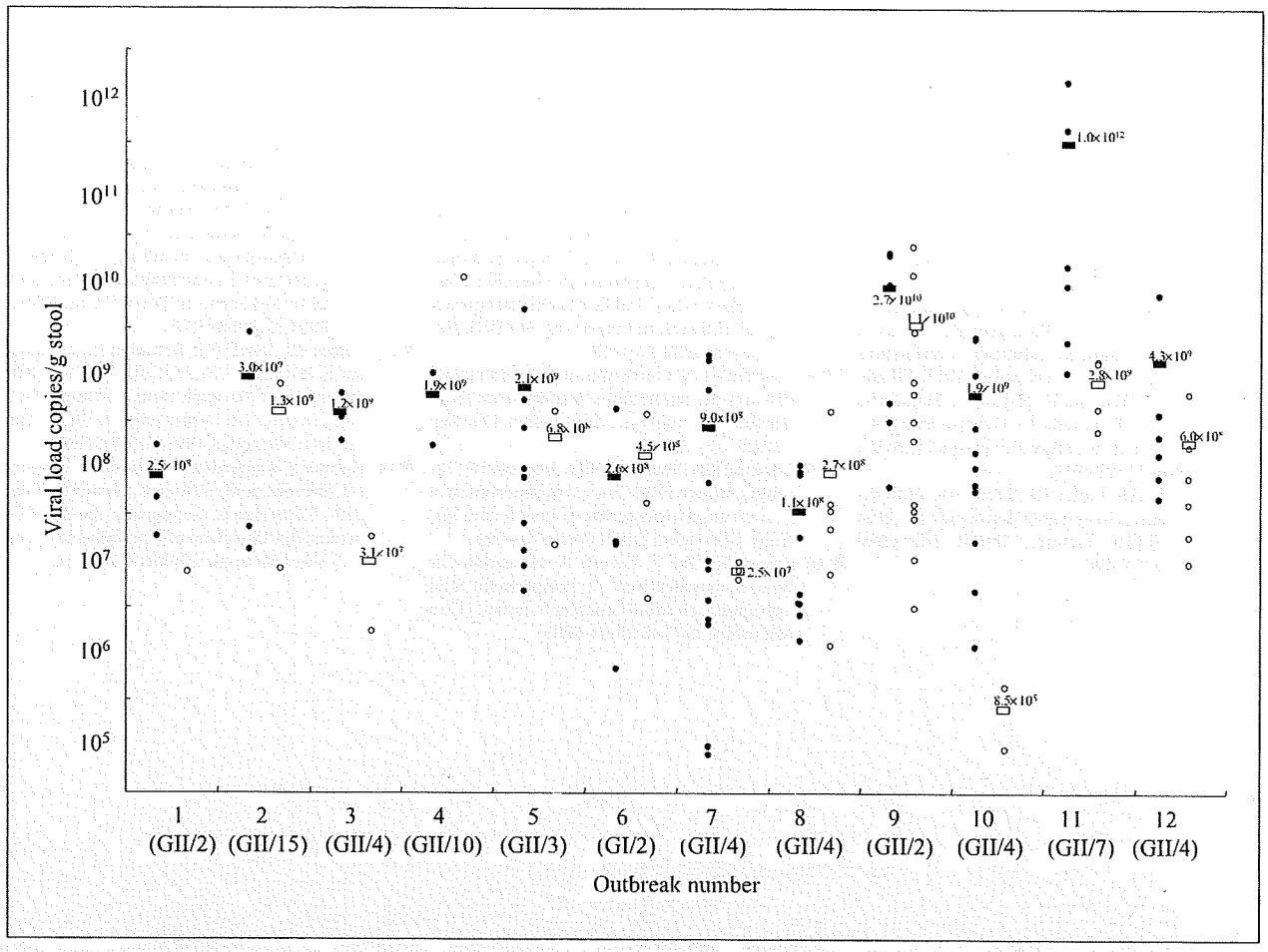

Fig. 2. Scatterplots of the viral loads in stool specimens from patients (●) and food handlers (○). Closed and open rectangles represent the median viral load from patients and food handlers, respectively. The median viral load for each genotype for the patients was 2.6×10^8, 8.9×10^{10}, 1.8×10^{10}, 2.1×10^9, 1.5×10^9, 1.0×10^{12}, 1.9×10^9 and 3.0×10^9 copies/g of stool for GI/2, GII/1, GII/2, GII/3, GII/4, GII/7, GII/10 and GII/15, respectively, whereas for symptomatic food handlers it was 4.5×10^8, 4.6×10^9, 1.0×10^{10}, 6.7×10^8, 2.5×10^8, 2.8×10^9 and 1.3×10^9 copies/g of stool for GI/2, GII/1, GII/2, GII/3, GII/4, GII/7 and GII/15, respectively.

Although detailed scientific information regarding NoV infection and its molecular epidemiology may have been limited in the present study, this report provides significant information regarding the molecular characterization of NoV causing gastroenteritis outbreaks in a particular setting in Japan. This is relevant in the field of NoV infection since the molecular epidemiology of the virus and its viral strains have been further clarified. To better understand the molecular epidemiology of NoV, it is imperative to analyze a larger number of cases of NoV outbreaks.

Acknowledgement

We thank Prof. Yutaka Inaba at Juntendo University School of Medicine for his helpful discussion.

References

1 Kageyama T, Kojima S, Shinohara M, Uchida K, Fukushi S, Hoshino FB, Takeda N, Katayama K: Broadly reactive and highly sensitive assay for Norwalk-like viruses based on real-time quantitative reverse transcription-PCR. J Clin Microbiol 2003;41:1548–1557.

2 Zheng DP, Ando T, Fankhauser RL, Beard RS, Glass RI, Monroe SS: Norovirus classification and proposed strain nomenclature. Virology 2006;346:312–323.

3 Hansman GS, Natori K, Shirato-Horikoshi H, Ogawa S, Oka T, Katayama K, Tanaka T, Miyoshi T, Sakae K, Kobayashi S, Shinohara M, Uchida K, Sakurai N, Shinozaki K, Okada M, Seto Y, Kamata K, Nagata N, Tanaka K, Miyamura T, Takeda N: Genetic and antigenic diversity among noroviruses. J Gen Virol 2006;87:909–919.

4 Hutson AM, Atmar RL, Estes MK: Norovirus disease: changing epidemiology and host susceptibility factors. Trends Microbiol 2004;12:279–287.

5 Koopmans M, Duizer E: Foodborne viruses: an emerging problem. Int J Food Microbiol 2004;90:23–41.

6 Lopman BA, Reacher MH, Van Duijnhoven Y, Hanon FX, Brown D, Koopmans M: Viral gastroenteritis outbreaks in Europe, 1995–2000. Emerg Infect Dis 2003;9:90–96.

7 Parashar U, Quiroz ES, Mounts AW, Monroe SS, Fankhauser RL, Ando T, Noel JS, Bulens SN, Beard SR, Li JF, Bresee JS, Glass RI: 'Norwalk-like viruses'. Public health consequences and outbreak management. MMWR Recomm Rep 2001;50:1–17.

8 Lawrence DN: Outbreaks of gastrointestinal diseases on cruise ships: lessons from three decades of progress. Curr Infect Dis Rep 2004;6:115–123.

9 Lopman BA, Reacher MH, Vipond IB, Sarangi J, Brown DW: Clinical manifestation of norovirus gastroenteritis in health care settings. Clin Infect Dis 2004;39:318–324.

10 Ozawa K, Oka T, Takeda N, Hansman GS: Norovirus infections in symptomatic and asymptomatic food-handlers in Japan. J Clin Microbiol 2007;45:3996–4005.

11 Gallimore CI, Cheesbrough JS, Lamden K, Bingham C, Gray JJ: Multiple norovirus genotypes characterised from an oyster-associated outbreak of gastroenteritis. Int J Food Microbiol 2005;103:323–330.

12 Kageyama T, Shinohara M, Uchida K, Fukushi S, Hoshino F B, Kojima S, Takai R, Oka T, Takeda N, Katayama K: Coexistence of multiple genotypes, including newly identified genotypes, in outbreaks of gastroenteritis due to Norovirus in Japan. J Clin Microbiol 2004;42:2988–2995.

13 Atmar RL, Neill FH, Romalde JL, Le Guyader F, Woodley CM, Metcalf TG, Estes MK: Detection of Norwalk virus and hepatitis A virus in shellfish tissues with the PCR. Appl Environ Microbiol 1995;61:3014–3018.

14 Kojima S, Kageyama T, Fukushi S, Hoshino FB, Shinohara M, Uchida K, Natori K, Takeda N, Katayama K: Genogroup-specific PCR primers for detection of Norwalk-like viruses. J Virol Methods 2002;100:107–114.

Jpn. J. Infect. Dis., 62, 63-66, 2009

Short Communication

Detection of Multiple Sapovirus Genotypes and Genogroups in Oyster-Associated Outbreaks

Reiko Nakagawa-Okamoto†*, Tomoko Arita-Nishida†**, Shoichi Toda, Hirotomo Kato[1], Hiroyuki Iwata[1], Miho Akiyama[2], Osamu Nishio[2], Hirokazu Kimura[2], Mamoru Noda[3], Naokazu Takeda[4], and Tomoichiro Oka[4]

Yamaguchi Prefectural Institute of Public Health and Environment, Yamaguchi 753-0821; [1]Department of Veterinary Hygiene, Yamaguchi University, Yamaguchi 753-8515; [2]Infectious Disease Surveillance Center and [4]Department of Virology II, National Institute of Infectious Diseases, Tokyo 208-0011; and [3]National Institute of Health Sciences, Tokyo 158-8501, Japan

(Received August 4, 2008. Accepted November 17, 2008)

SUMMARY: This report describes multiple viruses in stool specimens from oyster-associated gastroenteritis. Eleven outbreaks of oyster-associated gastroenteritis were examined for enteric viruses between January 2002 and March 2006 in Japan. Multiple norovirus genotypes were detected in all outbreaks; moreover, kobuvirus, sapovirus, and astrovirus were also detected in 6, 3, and 1 of the 11 outbreaks, respectively. Notably, multiple sapovirus genogroups were detected in the stool specimens from subjects in two oyster-associated gastroenteritis outbreaks.

Viral agents of gastroenteritis affect millions of people of all ages worldwide. The major viral agents of gastroenteritis include norovirus, sapovirus, rotavirus, astrovirus, and adenovirus (1,2). Kobuvirus, which is now classified into the family *Picornaviridae*, was also recently identified as a possible pathogen for gastroenteritis (3,4). Noroviruses are the dominant cause of gastroenteritis outbreaks worldwide, and are transmitted through the ingestion of contaminated foods, through the air, and by person-to-person contact (5-7). The majority of human noroviruses can be divided into two genogroups (GI and GII) (8). Recent reports revealed sapovirus to be an important cause of gastroenteritis outbreaks (9-13), although foodborne transmission of sapovirus has not been clearly demonstrated. Sapovirus can be divided into five genogroups (GI to GV), among which GI, GII, GIV, and GV are known to be human pathogens (14,15).

The purposes of this study were to detect norovirus, sapovirus, kobuvirus, and astrovirus in stool specimens collected from subjects in oyster-associated outbreaks of gastroenteritis, and then to address the genetic diversity of norovirus and sapovirus.

Stool specimens were collected from 56 patients and 15 food handlers in 11 oyster-associated outbreaks of gastroenteritis (i.e., outbreaks in which oysters were suspected to be the cause, since all affected individuals consumed or handled oysters) between January 2002 and March 2006 in Japan. This included seven restaurants, three private homes, and a monastery (Table 1). Nucleic acids were extracted from 140 μl of a 10% (w/v) stool suspension with a QIAamp Viral RNA kit (QIAGEN K. K., Tokyo, Japan) according to the manufacturer's protocol, and reverse transcription and reverse transcription-polymerase chain reaction (RT-PCR) were performed as previously described (16). Briefly, for norovirus GI PCR, G1SKF and G1SKR primers were used; and for norovirus GII PCR, G2SKF and G2SKR primers were used (16). For sapovirus, F13, F14, R13, and R14 primers were used to amplify the 1st PCR product, whereas for the nested PCR, F22 and R2 primers were used (17). For kobuvirus, C94b and 264K primers were used, and these were designed to amplify the 3C/D junction (3). For astrovirus, PreCAP1 and 12Gr primers were used to amplify the 1st PCR product, and then Mon244 and 82b primers were used for the nested PCR (18,19). Kobuvirus- and astrovirus-positive specimens were directly sequenced, whereas norovirus and sapovirus specimens were cloned into the pCR2.1 vector (Invitrogen Japan K. K., Tokyo, Japan), and at least four clones from each specimen were sequenced. Nucleotide sequences were determined as described earlier (20). The norovirus and sapovirus sequences determined in this study were registered as EF630535-EF630617 in DDBJ.

Forty-nine of 56 (88%) stool specimens from the patients and 6 of 15 (40%) stool specimens from food handlers were positive for at least one type of virus. Interestingly, about one-third of the specimens (21 of 71 [30%]) were positive for two or more types of viruses (Table 1). Noroviruses were detected in all 11 outbreaks, including 52 of 71 (73%) stool specimens. Norovirus GI sequences were detected in 3 of 11 outbreaks, whereas we detected both norovirus GI and GII sequences in the remaining eight outbreaks. The norovirus GI sequences were separated into 10 genotypes (GI/1-5, GI/8, GI/10, and GI/13-15), while the norovirus GII sequences were separated into six genotypes (GII/3-6, GII/8, and GII/12) (Fig. 1A). Two or more genotypes of noroviruses were detected in 20 of 52 (38%) norovirus-positive specimens (Table 1).

Sapoviruses were detected in 3 of 11 outbreaks, including 5 of 71 (7%) specimens. The sapovirus sequences belonged to GI/1, GII/1, GII/2, and GII/3 (Fig. 1B). Interestingly, we detected two sapovirus genogroups in one stool specimen: SAV-H2a (GII/2) and SAV-H2b (GI/1). Kobuviruses were

*Corresponding author: Mailing address: Yamaguchi Prefectural Institute of Public Health and Environment, 2-5-67 Aoi, Yamaguchi 753-0821, Japan. Tel: +81-83-922-7630, Fax: +81-83-922-7632, E-mail: okamoto.reiko@pref.yamaguchi.lg.jp

** Present address: National Institute of Infectious Diseases, Tokyo 208-0011, Japan.

†These authors contributed equally to this study.

Table 1. Details of the outbreaks showing the setting, no. of persons with symptoms and the viruses detected

Outbreak code	M/D/Y	Setting	No. persons with symptoms	No. specimens collected	Case	Symptoms	Norovirus (genogroup/ genotype)	Sapovirus (genogroup/ genotype)	Kobuvirus	Astrovirus
1	01.23.02	Home	5	3	individual	+	H1 (GI/4)	SAV-H1 (GII/2)	–	–
	01.23.02				individual	+	H2 (GI/4)	–	–	–
	01.23.02				individual	+	H3 (GI/2)	SAV-H2a (GII/2), SAV-H2b (GI/1)	–	–
2	01.23.02	Restaurant	16	14	individual	+	I1 (GII/12)	–	–	–
	01.24.02				individual	+	–	–	+	–
	01.24.02				individual	+	I3a (GI/13), I3b (GI/4)	–	–	–
	01.24.02				individual	+	I4 (GI/13)	–	–	–
	01.24.02				individual	+	–	–	–	–
	01.24.02				individual	+	–	–	–	–
	01.24.02				individual	+	I7 (GII/12)	–	+	–
	01.24.02				individual	+	–	–	–	–
	01.24.02				individual	+	–	–	–	–
	01.24.02				food-handler	–	I10a (GI/4), I10b (GI/13)	–	–	–
	01.24.02				food-handler	–	–	–	–	–
	01.24.02				food-handler	–	–	–	–	–
	01.24.02				individual	+	I13 (GII/12)	–	–	–
	01.24.02				individual	+	I14 (GII/12)	–	–	–
3	01.30.02	Restaurant	39	2	individual	+	J1 (GI/2), J1 (GII/12)	–	–	–
	01.25.02				individual	+	J2 (GII/5)	–	–	–
4	02.26.02	Home	8	4	individual	+	K1 (GII/5)	–	–	–
	02.28.02				individual	+	K2 (GII/5)	–	–	–
	03.01.02				individual	+	K3 (GII/3)	–	–	–
	03.01.02				individual	+	K4 (GI/4)	–	–	–
5	12.25.02	Home	5	4	individual	+	L1a (GI/15), L1b (GI/8), L1a (GII/4), L1b (GII/8)	–	+	–
	12.25.02				individual	+	L2a (GI/10), L2b (GI/13), L2c (GI/4)	–	–	–
	12.25.02				individual	+	L3 (GI/14), L3 (GII/3)	SAV-L3 (GI/1)	–	–
	12.25.02				individual	+	L4 (GI/14), L4 (GII/5)	–	+	–
6	02.07.03	Restaurant	3	4	individual	+	N1 (GI/8)	–	+	–
	02.07.03				individual	+	N2 (GI/4)	SAV-N4 (GII/3)	–	–
	02.07.03				individual	+	N3 (GI/4)	SAV-N5 (GII/1)	–	–
	02.09.03				food-handler	–	–	–	+	–
7	02.16.03	Restaurant	5	3	individual	+	O1 (GI/8), O1 (GII/6)	–	+	–
	02.17.03				food-handler	–	O2a (GI/1), O2b (GI/4)	–	+	–
	02.18.03				individual	+	O3a (GII/8), O3b (GII/6)	–	–	–
8	03.01.03	Restaurant	12	14	individual	+	P1a (GI/4), P1b (GI/8)	–	+	–
	03.01.03				individual	+	P2 (GI/8), P2 (GII/3)	–	+	–
	03.01.03				individual	+	P3 (GII/4)	–	+	–
	03.01.03				individual	+	P4a (GI/2), P4b (GI/8)	–	+	–
	03.01.03				individual	+	P5 (GII/5)	–	+	+
	03.01.03				food-handler	–	–	–	–	–
	03.01.03				food-handler	–	–	–	–	–
	03.01.03				food-handler	–	–	–	+	–
	03.01.03				food-handler	–	–	–	–	–
	03.01.03				food-handler	–	P10 (GI/1)	–	+	–
	03.01.03				food-handler	–	–	–	–	–
	03.01.03				food-handler	–	–	–	–	–
	03.01.03				food-handler	–	–	–	–	–
	03.01.03				individual	+	P14 (GI/2)	–	+	–
9	12.16.04	Monastery	9	4	individual	+	R1 (GI/3)	–	+	–
	12.18.04				individual	+	R2 (GI/3)	–	+	–
	12.17.04				individual	+	R3 (GI/1)	–	+	–
	12.18.04				individual	+	–	–	–	–
10	02.14.06	Restaurant	19	15	food-handler	–	S1 (GI/8)	–	–	–
	02.14.06				individual	+	S2 (GI/8), S2 (GII/4)	–	–	–
	02.14.06				individual	+	S3 (GII/3)	–	–	–
	02.14.06				individual	+	S4 (GI/8), S4 (GII/3)	–	–	–
	02.14.06				individual	+	S5 (GII/3)	–	–	–
	02.14.06				individual	+	S6 (GI/8)	–	–	–
	02.14.06				individual	+	S7 (GI/8)	–	–	–
	02.14.06				individual	+	S8 (GI/8), S8 (GII/6)	–	–	–
	02.14.06				individual	+	S9 (GII/5)	–	–	–
	02.14.06				individual	+	S10 (GI/8), S10 (GII/3)	–	–	–
	02.14.06				individual	+	S11 (GII/4)	–	–	–
	02.14.06				individual	+	S12a (GI/14), S12b (GI/5), S12a (GII/3), S12b (GII/5)	–	–	–
	02.14.06				individual	+	–	–	–	–
	02.14.06				individual	+	S14 (GI/8)	–	–	–
	02.14.06				individual	+	–	–	–	–
11	03.07.06	Restaurant	11	4	food-handler	–	–	–	–	–
	03.07.06				individual	+	T2a (GI/8), T2b (GI/3)	–	–	–
	03.07.06				individual	+	T3 (GI/8)	–	–	–
	03.07.06				individual	+	T4 (GI/8), T4 (GII/3)	–	–	–
Total				71			52	5	19	1

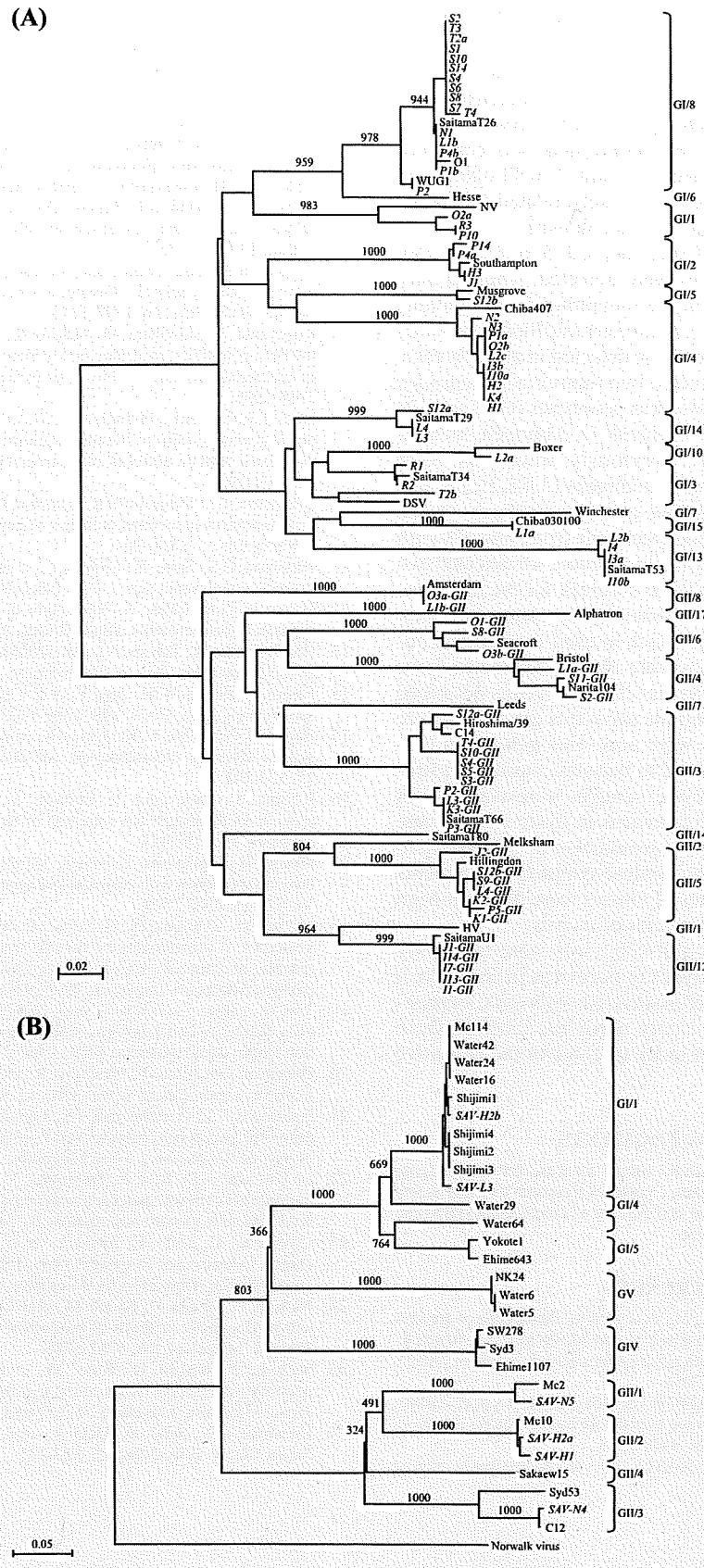

Fig. 1. Phylogenetic tree of the noroviruses (A) and sapoviruses (B) detected in this study. The trees were constructed with the partial N-terminal capsid region. The numbers on the branches indicate the bootstrap values for the clusters. Sequences and accession numbers from references (8) and (26), and Chiba030100 (AJ844469), Hiroshima/39 (AB262170), and C14 (AY845056) were used as the reference sequences.

detected in 6 of 11 outbreaks, including 19 of 71 (27%) specimens (Table 1). The kobuvirus sequences belonged to genotype A and shared greater than 98% nucleotide identity. Interestingly, 16 of 19 kobuvirus-positive specimens were also norovirus-positive, which suggests that co-contamination of these viruses in the natural environment was common. However, astrovirus was detected in only 1 of 11 outbreaks, and its nucleotide sequence was closely related to that of human serotype 4 sequences (data not shown).

In 7 of the 11 outbreaks (Outbreaks 1, 2, 5, 6, 7, 8, and 9), two or more types of viruses were detected, whereas only noroviruses were detected in the remaining four outbreaks (Outbreaks 3, 4, 10, and 11). Moreover, multiple norovirus genogroups and/or genotypes were detected in all outbreaks. It is noteworthy that we detected two sapovirus genogroups (GI/1 and GII/2) and two norovirus genotypes (GI/2 and GI/4) in one outbreak (Table 1, Outbreak 1). Although multiple norovirus genotypes were previously found, as were kobuviruses in oyster-associated outbreaks (3,4,8,21,22), this is the first report to detect multiple genotypes and genogroups of human sapoviruses in stool specimens from subjects with oyster-associated gastroenteritis. In addition, we detected two sapovirus genogroups in the same outbreak for the first time. Recently, we detected sapoviruses in the clam *Corbicula japonica* (bivalve mollusk), which is used for human consumption, and the sequences were closely related to those from patients with gastroenteritis (20). The results described in this study suggest that multiple sapovirus genotypes were concentrated in oysters, as were norovirus genotypes (23-25), which may be transmitted to humans, causing gastroenteritis. Unfortunately, no oyster samples were available for screening. The detection of sapovirus in oysters is an issue to be addressed in the future. It would also be interesting to determine whether or not the clinical symptoms of patients infected with multiple species of viruses were different from those infected with a single species of a virus.

In conclusion, sapovirus and kobuvirus were frequently detected with multiple genotypes of norovirus in stool specimens from subjects in oyster-associated outbreaks, suggesting that examination of not only norovirus but also these enteric viruses is needed in order to confirm the causative agents.

ACKNOWLEDGMENTS

This work was supported in part by a grant for Research on Emerging and Re-emerging Infectious Diseases, a grant for Research on Food Safety from the Ministry of Health, Labour and Welfare of Japan, and a grant from the Japan Health Science Foundation.

REFERENCES

1. Bon, F., Fascia, P., Dauvergne, M., et al. (1999): Prevalence of group A rotavirus, human calicivirus, astrovirus, and adenovirus type 40 and 41 infections among children with acute gastroenteritis in Dijon, France. J. Clin. Microbiol., 37, 3055-3058.
2. Sdiri-Loulizi, K., Gharbi-Khelifi, H., de Rougemont, A., et al. (2008): Acute infantile gastroenteritis associated with human enteric viruses in Tunisia. J. Clin. Microbiol., 46, 1349-1355.
3. Yamashita, T., Sugiyama, M., Tsuzuki, H., et al. (2000): Application of a reverse transcription-PCR for identification and differentiation of Aichi virus, a new member of the Picornavirus family associated with gastroenteritis in humans. J. Clin. Microbiol., 38, 2955-2961.
4. Ambert-Balay, K., Lorrot, M., Bon, F., et al. (2008): Prevalence and genetic diversity of Aichi virus strains in stool samples from community and hospitalized patients. J. Clin. Microbiol., 46, 1252-1258.
5. Gotz, H., de, J.B., Lindback, J., et al. (2002): Epidemiological investigation of a food-borne gastroenteritis outbreak caused by Norwalk-like virus in 30 day-care centres. Scand. J. Infect. Dis., 34, 115-121.
6. Marks, P.J., Vipond, I.B., Regan, F.M., et al. (2003): A school outbreak of Norwalk-like virus: evidence for airborne transmission. Epidemiol. Infect., 131, 727-736.
7. Centers for Disease, Control and Prevention (2008): Norovirus outbreak in an elementary school—District of Columbia, February 2007. Morb. Mortal. Wkly. Rep., 56, 1340-1343.
8. Kageyama, T., Shinohara, M., Uchida, K., et al. (2004): Coexistence of multiple genotypes, including newly identified genotypes, in outbreaks of gastroenteritis due to *Norovirus* in Japan. J. Clin. Microbiol., 42, 2988-2995.
9. Noel, J.S., Liu, B.L., Humphrey, C.D., et al. (1997): Parkville virus: a novel genetic variant of human calicivirus in the Sapporo virus clade, associated with an outbreak of gastroenteritis in adults. J. Med. Virol., 52, 173-178.
10. Johansson, P.J., Bergentoft, K., Larsson, P.A., et al. (2005): A nosocomial sapovirus-associated outbreak of gastroenteritis in adults. Scand. J. Infect. Dis., 37, 200-204.
11. Hansman, G.S., Saito, H., Shibata, C., et al. (2007): Outbreak of gastroenteritis due to sapovirus. J. Clin. Microbiol., 45, 1347-1349.
12. Hansman, G.S., Ishida, S., Yoshizumi, S., et al. (2007): Recombinant sapovirus gastroenteritis, Japan. Emerg. Infect. Dis., 13, 786-788.
13. Wu, F.T., Oka, T., Takeda, N., et al. (2008): Acute gastroenteritis caused by GI/2 sapovirus, Taiwan, 2007. Emerg. Infect. Dis., 14, 1169-1171.
14. Farkas, T., Zhong, W.M., Jing, Y., et al. (2004): Genetic diversity among sapoviruses. Arch. Virol., 149, 1309-1323.
15. Hansman, G.S., Oka, T., Katayama, K., et al. (2007): Human sapoviruses: genetic diversity, recombination, and classification. Rev. Med. Virol., 17, 133-141.
16. Kojima, S., Kageyama, T., Fukushi, S., et al. (2002): Genogroup-specific PCR primers for detection of Norwalk-like viruses. J. Virol. Methods, 100, 107-114.
17. Okada, M., Yamashita, Y., Oseto, M., et al. (2006): The detection of human sapoviruses with universal and genogroup-specific primers. Arch. Virol., 151, 2503-2509.
18. Matsui, M., Ushijima, H., Hachiya, M., et al. (1998): Determination of serotypes of astroviruses by reverse transcription-polymerase chain reaction and homologies of the types by the sequencing of Japanese isolates. Microbiol. Immunol., 42, 539-547.
19. Yan, H., Yagyu, F., Okitsu, S., et al. (2003): Detection of norovirus (GI, GII), Sapovirus and astrovirus in fecal samples using reverse transcription single-round multiplex PCR. J. Virol. Methods, 114, 37-44.
20. Hansman, G.S., Oka, T., Okamoto, R., et al. (2007): Human sapovirus in clams, Japan. Emerg. Infect. Dis., 13, 620-622.
21. Gallimore, C.I., Cheesbrough, J.S., Lamden, K., et al. (2005): Multiple norovirus genotypes characterised from an oyster-associated outbreak of gastroenteritis. Int. J. Food Microbiol., 103, 323-330.
22. Le Guyader, F.S., Bon, F., DeMedici, D., et al. (2006): Detection of multiple noroviruses associated with an international gastroenteritis outbreak linked to oyster consumption. J. Clin. Microbiol., 44, 3878-3882.
23. Costantini, V., Loisy, F., Joens, L., et al. (2006): Human and animal enteric caliciviruses in oysters from different coastal regions of the United States. Appl. Environ. Microbiol., 72, 1800-1809.
24. Nishida, T., Kimura, H., Saitoh, M., et al. (2003): Detection, quantitation, and phylogenetic analysis of noroviruses in Japanese oysters. Appl. Environ. Microbiol., 69, 5782-5786.
25. Nishida, T., Nishio, O., Kato, M., et al. (2007): Genotyping and quantitation of noroviruses in oysters from two distinct sea areas in Japan. Microbiol. Immunol., 51, 177-184.
26. Hansman, G.S., Sano, D., Ueki, Y., et al. (2007): Sapovirus in water, Japan. Emerg. Infect. Dis., 13, 133-135.

JOURNAL OF VIROLOGY, Feb. 2007, p. 1119–1128 Vol. 81, No. 3
0022-538X/07/$08.00+0 doi:10.1128/JVI.01909-06

Presence of a Surface-Exposed Loop Facilitates Trypsinization of Particles of Sinsiro Virus, a Genogroup II.3 Norovirus[▽]

Shantanu Kumar,[1] Wendy Ochoa,[1] Shinichi Kobayashi,[2] and Vijay S. Reddy[1]*

Department of Molecular Biology, The Scripps Research Institute, 10550 North Torrey Pines Road, La Jolla, San Diego, California 92037,[1] and Laboratory of Virology, Aichi Prefectural Institute of Public Health, Nagoya, Aichi 462-8576, Japan[2]

Received 1 September 2006/Accepted 25 October 2006

Noroviruses (NoVs) are the causative agents of nonbacterial acute gastroenteritis in humans. NoVs that belong to genogroup II (GII) are quite prevalent and prone to undergo recombination, and their three-dimensional structure is not yet known. Protein homology modeling of Sinsiro virus (SV), a member of the GII.3 NoVs, revealed the presence of a surface-exposed 20-amino-acid (aa) insertion in the P2 domain of the capsid protein (CP) relative to the Norwalk virus (NV) CP, which is a well known hot spot for mutations to counter the host immunological response. To further characterize the role of the long insertion in SV, the capsid protein gene was expressed using the recombinant baculovirus system. Trypsinization of the resultant virus-like particles yielded two predominant bands (31.7 and 26.1 kDa) in sodium dodecyl sulfate-polyacrylamide gel electrophoresis and Western blot analysis. N-terminal sequencing and analysis of the mass spectroscopic data indicated that these fragments correspond to residues 1 to 292 (26.1 kDa) and 307 to 544 (31.7 kDa). In addition, the above data taken together with the comparative modeling studies indicated that the trypsin cleavage sites of the Sinsiro virus CP, Arg292 and Arg307, are located at the beginning of and within the 20-aa insertion in the P2 domain, respectively. This study demonstrates that the presence of the surface-exposed loop in the GII.3 NoVs facilitates the trypsinization of the capsid protein in the assembled form. The SV particles remain intact even after trypsin digestion and retain the suggested receptor binding linear epitope of residues 325 to 334. The above results are distinct from those obtained from the trypsinization studies performed earlier on the NV (GI) and VA387 (GII) viruses, both of which lack the large surface insertion and associated basic residues. These new observations may have implications for host receptor binding, cell entry, and norovirus infection in general.

Human noroviruses (NoVs) are causative agents of nonbacterial acute gastroenteritis, second only to rotaviruses, in all age groups of humans and are associated with significant morbidity worldwide and substantial mortality in developing countries (12, 15, 21, 25). They belong to the genus *Norovirus* in the family *Caliciviridae*. The rates of infection with NoVs are high, and the viruses spread rapidly from person to person primarily via the fecal-oral route, resulting in large outbreaks of disease that often persist. The magnitude of genetic and antigenic diversity among NoV strains came to light in the past several years due to greater surveillance of disease outbreaks and rapid availability and analysis of sequence data (1, 12, 13, 24, 38, 41). The NoV strains that infect humans are classified into two major genogroups, genogroup I (GI) and GII. The GII strains exhibit greater virulence, as they are prone to undergo recombination, and they cause the majority of gasteroenteritis worldwide (14, 19, 22, 30, 31, 42).

NoVs are spherical with a diameter of ~35 nm and contain a single-stranded, positive-sense, polyadenylated RNA genome of 7,400 to 7,700 nucleotides (2). The genome is divided into three open reading frames (ORFs). ORF1 encodes a 200-kDa polyprotein, which is further processed into at least six nonstructural proteins. ORF2 codes for the ~60-kDa capsid protein (CP) VP1, and ORF3 encodes a minor structural protein, VP2, which is basic in nature (15, 28). Studies on the life cycle and pathogenesis of NoVs have been hampered by the lack of an appropriate cell culture system. However, the ability to generate virus-like particles (VLPs) from insect cells infected with recombinant baculoviruses expressing the coat protein (VP1) and in vitro studies of binding to histo-blood group antigens has led to significant advances related to NoV structure, function, and biophysical properties (3, 7, 20, 29).

The three-dimensional (3D) structures of Norwalk virus (NV) VLPs and San Miguel sea lion virus, a member of the genus *Vesivirus* (GII.2) in the family *Caliciviridae*, have been determined at near-atomic resolution (10, 29). Typically, NV capsids are composed of 180 copies of a coat protein (VP1) assembled into T = 3 icosahedral virions. However, it has been reported that sometimes VP1 subunits form smaller capsids, which consists of 60 subunits with T = 1 icosahedral symmetry (40). The tertiary structure of the NV capsid protein contains two major structural domains: the shell (S) domain with a canonical β-barrel fold and the protruding (P) domain. The S domain consists of the N-terminal 225 amino acids (aa), and the P domain is composed of 226 to 530 aa. The P domain is further divided into two subdomains, P1 and P2. The P1 domain comprises aa 226 to 278 and 406 to 530. The P2 domain is a 127-aa insertion (aa 279 to 405) in the P1 domain; it is the most distal part of the folded coat protein (VP1) and is located at the exterior surface of the capsid (29). The P2 domain is therefore predicted to contain the antigenic determinants of the immunological response of the host. A binding surface that

* Corresponding author. Mailing address: Department of Molecular Biology, TPC-6, The Scripps Research Institute, 10550 North Torrey Pines Road, La Jolla, CA 92037. Phone: (858) 784-8191. Fax: (858) 784-8688. E-mail: reddyv@scripps.edu.

▽ Published ahead of print on 1 November 2006.

interacts with the human histo-blood group antigens was mapped onto the P2 domain by computational analysis and later confirmed by site-directed mutagenesis (35). Recently, Lochridge et al. identified amino acids 291 to 293 and 313 to 322 as the likely antigenic epitopes in the P2 domains of NV and Snow Mountain virus, which are the reference strains of GI.1 and GII.2, respectively (23). The linear epitope composed of amino acids 313 to 322 in Snow Mountain virus, which has been suggested to be responsible for the host cell interactions, is conserved among all the NoVs (23).

Sequence analysis of the NoV capsid protein indicated that the S-domain sequences are about 30% identical, while the sequence identity drops to 11% and 8% in the P1 and P2 domains, respectively (9). Even though there are many trypsin and chymotrypsin cleavage sites across the entire capsid protein, results obtained from the proteolytic analysis of the Norwalk virus VLPs clearly indicated that the intact NV particles are resistant to trypsin digestion (18). However, trypsin digestion of the soluble protein of NV resulted in partial digestion of the capsid protein, in which the S domain was completely digested while the P domain remained intact (18). These data indicated that the P-domain structure is resistant to proteases. However, recent studies by Tan et al. contradict the above results. In particular, they suggest that the intact particles of NV and VA387, a GII.4 virus, undergo partial trypsinization near the hinge region between the S and P domains, thereby releasing the nearly intact P domain of 32 to 34 kDa (36).

Sinsiro virus (SV), the subject of the present study, belongs to the GII.3 NoVs. The capsid protein of SV is made of 548 aa residues and exhibits 98% amino acid sequence identity with other members of GII.3 NoVs (e.g., Arg320, Oberhausewn, and Toronto viruses, etc.). The prevalence of acute gastroenteritis caused by these strains suggested that they have better adaptability to circumvent the human immune response (27). The molecular and structural characterization of SV VLPs may provide further insights into their pathogenesis. Here we report the results of studies on expression of the SV capsid protein in insect cells by using a recombinant baculovirus system, three-dimensional electron microscopy (EM) reconstruction using negatively stained particles, and homology modeling of the SV capsid. In addition, we characterized the unique trypsin cleavage pattern of SV by using N-terminal sequencing, mass spectrometry analysis, and molecular modeling studies. The sequence in and around the insertion is conserved among all GII.3 and GII.6 NoVs, suggesting that these viruses undergo similar patterns of trypsinization. The results from this study may provide some of the possible reasons for the greater efficacy of virus-cell interactions involving GII.3 and GII.6 NoVs.

MATERIALS AND METHODS

Homology modeling of the SV capsid. The comparative modeling program MODELLER (version 6.0) and the default modeling options (32) were used to generate homology models of Sinsiro virus. The Norwalk virus capsid structure (PDB no. 1IHM) was used as the template due to its having greater sequence identity (47%) than the San Miguel sea lion virus (PDB no. 2GH8), which has only 17% amino acid sequence identity with SV. The amino acid sequence identity of 47% between Sinsiro and Norwalk viruses is well above the threshold (35%) for obtaining a reliable homology model. A multiple-sequence alignment was obtained by aligning the amino acid sequences of 12 different NoVs, including Sinsiro virus, to the Norwalk virus sequence, using the Clustal-w server available at http://clustalw.genome.jp/. In addition, six neighboring subunits that immediately surround the three reference subunits (A, B, and C) (http://viperdb.scripps.edu/info_page.php?VDB = 1ihm) (34) were included to impose restraints on the subunit interfaces. At the end of the modeling run, the reference subunits (A, B, and C) were extracted and used for the subsequent analysis.

Cell culture. *Spodoptera frugiperda* cells (line IPLB-Sf21) were grown at 27°C in TC100 medium (Invitrogen, Carlsbad, CA) supplemented with 0.35 g of $NaHCO_3$ per liter, 2.6 g of tryptose broth per liter, 2 mM L-glutamine (final concentration), 100 U of penicillin per ml, 100 μg of streptomycin per ml, and 10% heat-inactivated fetal bovine serum (33). Cultures were maintained as monolayers in screw-cap plastic flasks or as suspensions in 1-liter spinner flasks. Hi5 cells were grown at 27°C in ESF 921 medium (Expression System, CA) supplemented with 100 μg of penicillin per ml and 100 μg of streptomycin per ml. Cultures were maintained in suspension on a shaker (100 rpm) in a 500-ml polypropylene bottle.

Generation of recombinant baculoviruses expressing SV coat protein. The cDNA clone of Sinsiro virus capsid protein was generously provided to us by Shinichi Kobayashi (Aichi Prefectural Institute of Public Health, Nagoya, Japan) and used as a template in a PCR to amplify the full-length capsid gene (GenBank accession no. AB195226), using forward (5′CGGGATCCATGAAGATGGCG TCGAATG3′) and reverse (5′GCTCTAGATTATTGAATCCTTCTACGCCC A3′) primers having 5′ BamHI and XbaI restriction sites, respectively. PCR was performed using high-fidelity *Pfx* polymerase (Invitrogen) according to the manufacturer's instructions. Recombinant baculovirus transfer plasmids (pBPSV) containing the full-length Sinsiro virus CP sequence were generated by inserting PCR-amplified fragments flanked by BamHI and XbaI restriction enzyme sites into the multiple cloning sites of pBacPAK9 (BD Biosciences-Clontech, CA). pBSV plasmids were sequenced using Bac1 (5′ACCATCTCGCAAATAAATA 3′) and Bac2 (5′CAACGCACAGAATCTAGCG 3′) primers to confirm the accuracy of the SV sequence. Recombinant baculoviruses expressing SV CPs were generated by cotransfecting pBPSV plasmids with linearized baculovirus DNA (pBacPAK6) according to the manufacturer's instructions (BD Biosciences-Clontech). Recombinant baculoviruses were plaque purified and amplified to obtain pure stocks of viruses.

Expression and purification of rSV particles. Recombinant SV (rSV) particles were prepared and purified essentially as previously described (17). Briefly, *Trichoplusia ni* (Tn5) insect cells (2.0×10^6 cells per ml) were infected with a baculovirus recombinant expressing the capsid protein of SV at a multiplicity of infection of 5 and incubated for 3 days at 27°C in a incubator shaker maintained at 100 rpm. Nonidet P-40 was added to a final concentration of 0.5% (vol/vol) and incubated on ice for 10 min to lyse the cells. rSV particles released into the medium were separated from the cell lysate by centrifuging the culture for 15 min at 10,000 rpm in a JA-17 rotor, using a Beckman J2-21 centrifuge. The expressed protein in supernatant was concentrated by precipitation with polyethylene glycol (8%) and was further purified by centrifugation through a 30% (wt/wt) sucrose cushion for 2 h in an Ti 50.2 rotor (Beckman) at 35,000 rpm. Pellets were suspended in 0.1 M phosphate buffer (pH 6.0), layered onto 10 to 40% sucrose gradients, and centrifuged for 3 h at 26,000 rpm in an SW28 rotor. Peak fractions then were pooled, dialyzed, and stored at 4°C. Integrity of the rSV VLPs was confirmed by EM observation of particles negatively stained with 1% uranyl acetate. The protein concentrations were determined with a Bradford assay kit for quick protein estimation (Bio-Rad).

Native gel analysis. The purified VLPs were subjected to native gel analysis in 0.5% (wt/vol) agarose gels with 0.1 M Tris-malate buffer (pH 6.5) containing 0.001% (wt/vol) ethidium bromide. The electrophoresis was carried out at a constant voltage (40 V) for 3 h, and RNA was visualized in a Bio-Rad Gel Doc system. The gel was dried and stained for protein with 0.05% (wt/vol) Coomassie brilliant blue R250.

Isolation of RNA from purified particles and reverse transcription-PCR analysis. Sodium dodecyl sulfate (SDS) and NaCl were added to gradient-purified SV particles at final concentrations of 1% (wt/vol) and 0.2 M, respectively. RNA was extracted with an equal volume of acidic phenol-chloroform and precipitated with 3 volumes of ethanol in the presence of 0.3 M sodium acetate and 20 mg of glycogen. After several hours at −20°C, the RNA was pelleted, washed with 70% ethanol, dried, and dissolved in nuclease-free water, and first-strand cDNA synthesis was carried out using CP-specific antisense primers with reverse transcriptase (Invitrogen, CA). The PCR was performed using *Pfx* polymerase (Invitrogen, CA).

Production of hyperimmune antiserum in laboratory mice and ELISA. To produce hyperimmune serum, mice were immunized with rSV capsid protein. The immunization regimen consisted of one intramuscular injection of the purified rSV in Freund's adjuvant (at a dose of 60 μg per mouse) followed by two

booster injections of the same dose in Freund's incomplete adjuvant. The animals were bled 2 weeks after the last booster injection. An enzyme-linked immunosorbent assay (ELISA) was performed to quantify the titer of antibody. Briefly, the VLPs were directly applied to microplates (nun-Immuno plates) at 100 μl per well and a final concentration of 1 μg/ml in carbonate-bicarbonate buffer (0.05 M, pH 9.6) and were incubated overnight at 4°C. The antigen-coated plates were blocked for 2 h at room temperature with 5% nonfat milk in 0.01 M phosphate-buffered saline (PBS) (pH 7.2) and washed thrice with PBS containing 0.05% Tween 20 (PBST). Different dilutions of primary antisera (1:10, 1:100, 1:1,000, and 1:10,000) were incubated with the antigen for 1 h at room temperature and washed thrice with PBST. Anti-mouse immunoglobulin (Sigma) was diluted 1:10,000, and the plates were incubated for 1 h at room temperature. Following incubation, the plates were washed thrice with PBST. 3,3′,5,5′-tetramethyl benzidine (TMB)–peroxidase substrate (Sigma) was added, and the color was allowed to develop for 10 min at room temperature. The reaction was stopped by adding 1% SDS, and the optical density at 405 nm was determined with a Spectra Max-250 (Molecular Devices, CA).

Trypsin digestion of assembled and solubilized rSV protein. TPCK (*N*-tosyl-L-phenylalanine chloromethyl ketone)-trypsin was purchased from Sigma-Aldrich. Stock solutions were prepared at concentrations of 2 mg/ml in 0.001 N HCl, and serial dilutions were made in PBS (pH 7.4). Digestions of rNV particles were performed for 30 min at 37°C in reaction volumes of 20 microliters. Following incubation, reaction products were electrophoresed on 4 to 12% bis-Tris gels (Invitrogen, CA), and bands were visualized by staining with Simple blue as described by the manufacturer (Invitrogen, CA). Disassociation of VLPs was performed by dialyzing rSV particles overnight at 4°C in 50 mM Tris (pH 8.9). Samples were also visualized under EM to confirm the disassembly of VLPs. Digestion of solubilized rSV protein was performed as described for the assembled particles.

Gradient purification of trypsin-digested rSV particles was done by treating the VLPs (1 mg/ml) with trypsin (62.5 μg/ml) at 37°C for 30 min in a reaction volume of 1.0 ml. This was followed by layering 500 μl of the digested VLPs on a continuous 10 to 40% sucrose gradient and centrifuging for 2 h in an SW41 rotor (Beckman), and fractions were collected by bottom puncture and analyzed by SDS-polyacrylamide gel electrophoresis (SDS-PAGE) and Western blot analysis.

SDS-PAGE and immunoblotting analysis. Samples to be analyzed were boiled for 2 min in sample buffer containing 2% SDS, 100 mM dithiothreitol, 0.05 M Tris-HCl (pH 6.8), 10% glycerol, and 0.1% bromophenol blue. Proteins were analyzed on 4 to 12% bis-Tris gels according to the manufacturer's instructions (Invitrogen, CA). The proteins separated by SDS-PAGE were transferred onto a polyvinylidene difluoride (PVDF) membrane (Invitrogen, CA) as described by manufacturer. The full-length SV and trypsin-digested SV capsid protein were detected using a mouse hyperimmune anti-rSV serum at a dilution of 1:5,000 in PBS. The secondary antibodies used were conjugated to horseradish peroxidase (Chemicon International, CA). The membrane was developed with SuperSigna West Pico chemiluminescent substrate (Pierce Biotechnology, Inc., IL) according to the manufacturer's protocol.

Transmission EM (TEM). Negative-stain EM was used to analyze the presence, integrity, and morphology of the rSV VLPs. Uranyl acetate (1%; pH 5.0) was used to stain the samples. A drop of the sample (10 μl) was placed on glow-discharged, carbon-coated, 400-mesh copper grids (Ted Pella Inc., Redding, CA) for 1 min at room temperature. The grids were washed three times by being transferred into drops of water placed on Parafilm, and the excess liquid was blotted off from the side of the grid with a filter paper. The grids were then stained by quickly immersing them (twice) into drops of uranyl acetate solution and finally were placed in a third drop of uranyl acetate stain for 1 min, and excess liquid was blotted out as before. The grids were then air dried for 5 min at room temperature and examined under a CM100 microscope (Phillips) at 80 kV at a magnification of ×45,000, and photographs were recorded at a magnification of ×52,000.

Reconstruction of negatively stained VLPs. The VLP samples at a concentration of 4 mg/ml were placed on glow-discharged carbon film and stained briefly with 2% uranyl acetate. The grids were observed in a Philips Tecnai F20 transmission electron microscope operated at 120 kV. Digital images were recorded using low-irradiation procedures (20 electrons/Å^2), and those that displayed minimal astigmatism and drift as assessed by visual inspection and diffraction were selected for further analysis. Particles separated from their neighbors and with a clear background were selected and masked as individual images by using the software ROBEM (6). The image intensity values were adjusted to remove linear background gradients and to normalize the means and variances of the data (8). The initial orientation and origin parameters of the images for the reconstruction were determined by a model-based refinement approach. An electron density map was calculated from the X-ray coordinates of Norwalk virus (PDB no. 1IHM) and used as an initial model. The translation (x, y) and orientation $(0, 0, w)$ parameters were refined for each particle by use of repeated cycles of correlation procedures (4–6). Images were typically discarded if they showed a correlation coefficient, calculated between the raw image and the corresponding projected view of an intermediate reconstruction, of less than one standard deviation of the mean correlation coefficient of the entire data set. A complete refinement protocol was carried out using the EM3DR package (6). The final maps were computed using a total of 184 individual particles.

Mass spectrometry and N-terminal amino acid protein sequence analysis. The molecular weights of protein were determined by matrix-assisted laser desorption ionization–time-of-flight (MALDI-TOF) mass spectrometry performed at the core facility of the Scripps Research Institute, CA. For N-terminal amino acid sequence analysis, proteins separated by SDS-PAGE were transferred onto a PVDF membrane and stained with Ponceau red, and the bands corresponding to the trypsin cleavage products, detected by Western blot analysis, were excised. N-terminal microsequencing was performed on an Applied Biosystems (ABI Procise) protein sequencer in the Protein Sequencing Core Facility at the Scripps Research Institute.

RESULTS

Production of recombinant SV VLPs by using the baculovirus expression system. A PCR-amplified 1.7-kb fragment (ORF2 of SV) was subcloned into a baculovirus transfer vector to produce a construct called pBPSV. Sequencing of pBPSV confirmed the presence and accuracy of the SV sequence. Recombinant baculoviruses expressing the coat protein of SV were isolated by transfecting the Sf21 cells with pBPSV and linearized genomic DNA, followed by plaque purification. Electrophoretic analysis of the overexpressed proteins from the infected cells showed a major band with an apparent molecular mass of 60 kDa (data not shown). Recombinant Sinsiro virus VLPs were further purified by banding on a 10% to 40% sucrose gradient, and the peak fractions were collected. SDS-PAGE analysis of the fractions highlighted the presence of a single major band of ~60 kDa (Fig. 1A). Examination of the major peak fraction (Fig. 1A, lane 6) under a transmission electron microscope by employing negative-staining procedures confirmed the presence of intact particles (Fig. 1B). These particles resembled the typical NoV particles produced in earlier studies (20). We observed mostly empty particles, as seen in the case of NV VLPs, and a few full particles having an average diameter of ~35.0 nm. However, the relative proportions of the full and empty particles varied from one preparation to another and also depended on the type of insect cells (e.g., Sf21 or Tn5) used for the baculovirus expression. Although the formation of full capsids is not a very common observation, such a finding has been reported earlier in the case of Hawaii human calicivirus (GII) (16). The gradient-purified rSV particles were used for immunizing mice. The serum samples collected from the mice showed high titers of antibodies against rSV as evaluated by ELISA (data not shown).

EM reconstruction of negatively stained rSV capsids. Since our efforts to obtain good frozen cryosamples had not been very successful so far, a preliminary 3D reconstruction of VLPs was carried out using 186 negatively stained particles, which adequately sampled the icosahedral asymmetric unit to a resolution of 26 Å. The reconstruction clearly showed that the subunits are organized in a T = 3 icosahedral arrangement with a thin contiguous shell and distinctive protrusions on the

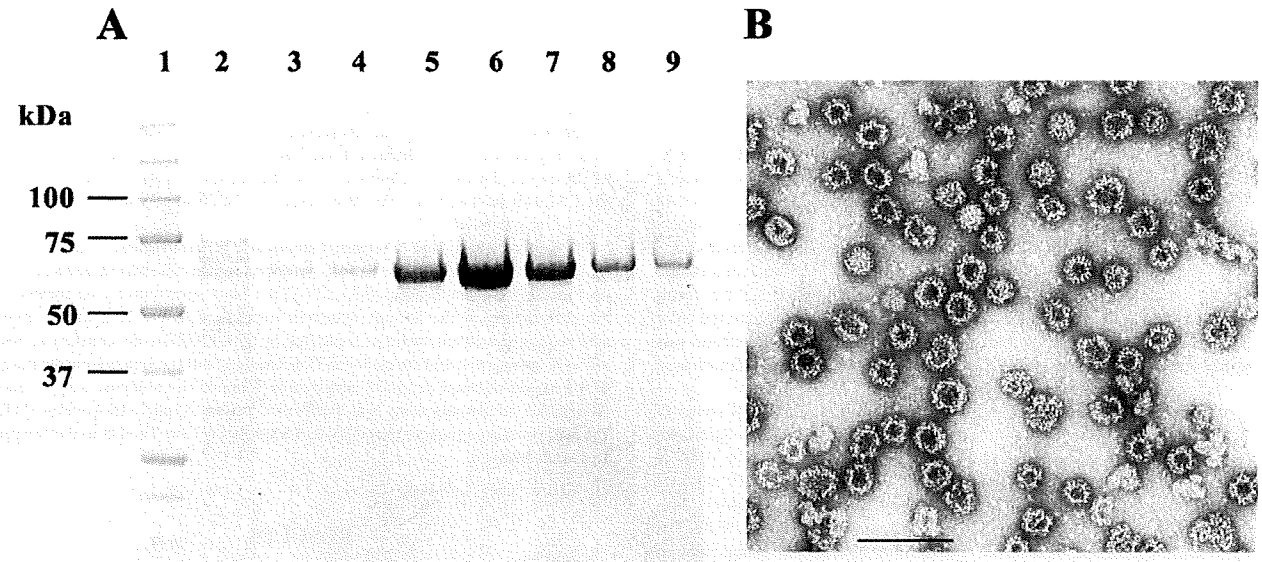

FIG. 1. SDS-PAGE analysis and electron micrographs of rSV VLPs. (A) SDS-PAGE analysis of the peak fractions of a sucrose gradient. Lane 1, molecular mass marker; lanes 2 to 9, fractions collected from the gradient. The arrow indicates a single major band of ~60 kDa. (B) Negative-stain electron microscopy of purified rSV VLPs, showing empty VLPs. Bar, 100 nm.

surface (Fig. 2A and B). A comparative analysis of this reconstruction with the 3D structure of the recombinant Norwalk virus (PDB-ID no. 1IHM) (29) showed no discernible differences at this resolution. The relative dispositions of the shell and the protruding domains appeared identical to those of Norwalk virus.

Characterization of RNA associated with VLPs. Purified rSV VLPs were analyzed on a native 0.5% agarose gel and stained with ethidium bromide to visualize the presence of RNA. The same gel was dried and stained for protein with Coomassie brilliant blue R-250. Interestingly, the VLPs stained positive for both RNA and protein (Fig. 3A and B).

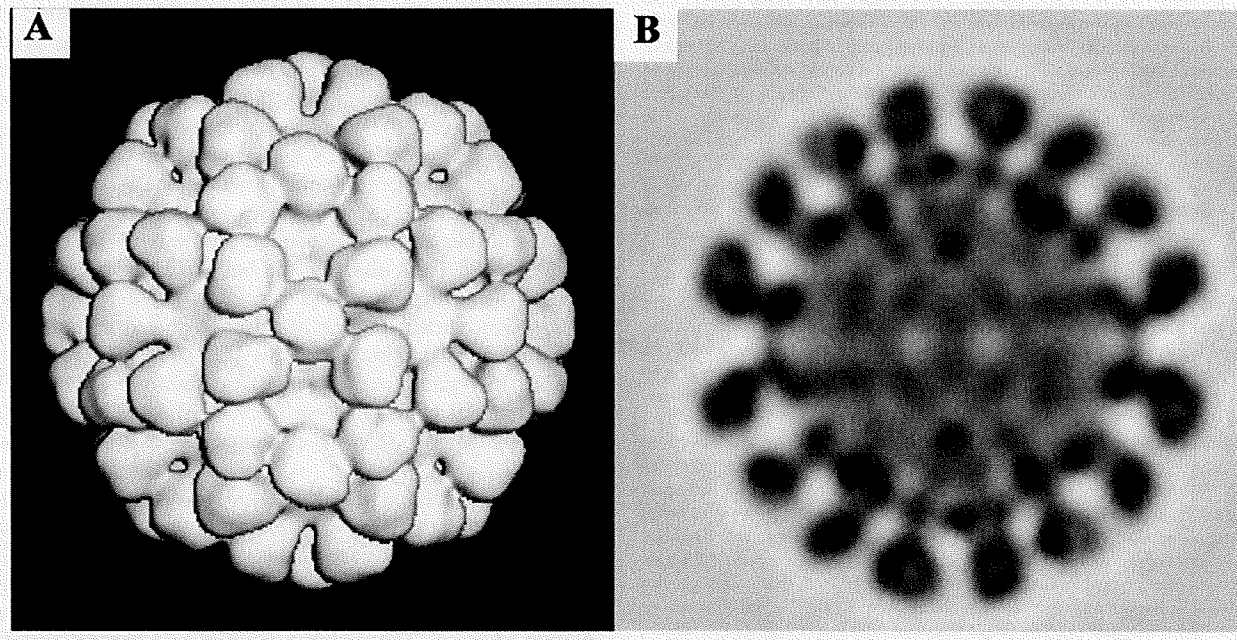

FIG. 2. Surface-shaded EM 3D density map of VLPs of SV viewed down the icosahedral twofold axis of symmetry (A) and the central section view through the 3D density map (B). The map was generated from individual 2D projections, which were manually selected from the digital micrographs of a negatively stained sample.

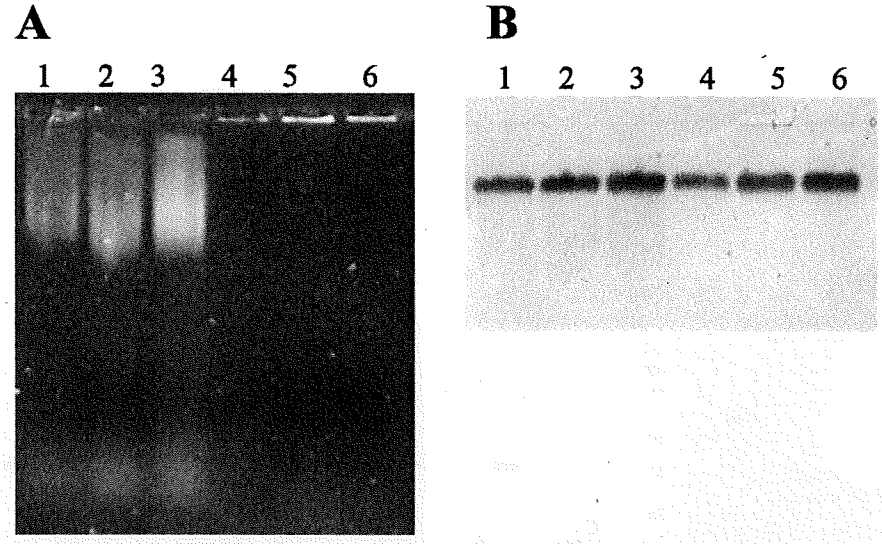

FIG. 3. Native agarose gel electrophoresis of rSV VLPs, followed by ethidium bromide staining. (A) Lanes 1 to 3, purified rSV VLPs (1 μg, 2 μg, and 3 μg, respectively); lanes 4 to 6, same as lanes 1 to 3, but samples were treated with RNase. (B) The same gel was dried and stained with Coomassie brilliant blue R-250.

This was rather surprising, as we saw mostly empty particles under the electron microscope (Fig. 1B). First-strand cDNA synthesis of the RNA isolated from the VLPs with murine leukemia virus reverse transcriptase and a capsid protein primer did not produce a PCR product, suggesting that the RNA is of cellular origin (data not shown). Interestingly, treatment of the VLPs with RNase resulted in complete degradation of RNA, indicating that the RNA was bound on the exterior surface of the rSV capsids rather than in particles encapsidating the RNA (Fig. 3A). It is also possible that the trace amounts of cellular RNA packaged into a small number of full particles could not be detected by ethidium bromide staining.

Trypsin digestion and MALDI-TOF analysis of rSV VLPs and soluble CP. Purified rSV particles were incubated with an equal volume of trypsin in serial twofold dilutions, beginning with the highest concentration of 500 μg/ml, for 30 min at 37°C. Two predominant cleavage products were observed on SDS-PAGE (Fig. 4A). MALDI-TOF analysis of the trypsin-treated VLPs revealed the mean molecular masses of these two fragments to be 26.1 and 31.7 kDa (Fig. 4B and C). To determine the exact sites of trypsinization, The VLPs were digested with trypsin, the proteolytic fragments were separated by gel electrophoresis, and the bands were transferred onto a PVDF membrane for N-terminal sequencing. Sequencing analysis of the first 10 amino acids of the 26.1-kDa cleavage product showed that the specific cleavage occurred at residue Arg307 of the rSV capsid protein (Fig. 5). Further analysis of the mass spectral data by using the proteomics tool at http://prospector.ucsf.edu/ucsfhtml4.0/msdigest.htm suggested that the 26.1-kDa band corresponds to residues 308 to 544. The last four residues from the C terminus (residue 548) could have been cleaved prior to or after the cleavage at residue 307. For unknown reasons, N-terminal sequencing of the 31.7-kDa band did not give conclusive results. However, the analysis using the proteomics tool suggested that the 31.7-kDa band might have resulted from trypsin cleavage at residue Arg292, and it corresponds to residues 1 to 292, encompassing the S domain and partial P domain. Assuming that the latter result was correct, it explains the difficulties in obtaining the N-terminal sequence of the 31.7-kDa fragment, perhaps due to possible N-terminal modifications. Interestingly, both these cleavage sites, Arg292 and Arg307, are located in and around the 20-aa insertion in the P2 domain. Even though the proteomics tool suggested that the 29.3-kDa peak found in the MALDI-TOF spectra (Fig. 4C) of the trypsin-digested soluble rSV coat protein corresponds to either residues 95 to 358 or 188 to 452, we did not further characterize this peak, as the corresponding band was not seen in SDS-PAGE or Western blot analysis.

To determine whether the 26.1- and 31.7-kDa bands were the result of trypsinization of intact VLPs or due to free subunits resulting from the disassembled capsids, SDS-PAGE and Western blot analysis of the peak fractions of the trypsin (62.5 μg/ml)-digested VLPs separated through sucrose gradients were performed. The fractions from the top of the gradient resulted in a single (26.1-kDa) band, whereas the fractions from the middle of the gradients showed both the 26.1-kDa and 31.7-kDa bands (Fig. 6A and B). Observation of both fractions by EM revealed the presence of VLPs only in the middle fractions (Fig. 6C). This clearly implies that the two (31.7-kDa and 26.1-kDa) bands are the result of trypsin digestion of the VLPs. Interestingly, the VLPs remain intact in sucrose for up to 72 h after undergoing trypsinization. On the other hand, trypsin digestion of the soluble rSV protein obtained by incubating VLPs in Tris buffer (pH 8.9) resulted in only the 26.1-kDa band at a lower concentration of trypsin (Fig. 7A and B). However, at a higher concentration of trypsin, the 26.1-kDa band was further cleaved to smaller peptides (data not shown).

Conservation of trypsin cleavage sites in human NoVs. Sequence alignment of these capsid proteins from various strains of NoVs suggested that approximately 48% of the amino acids in the S domain are conserved whereas fewer than 10% of the

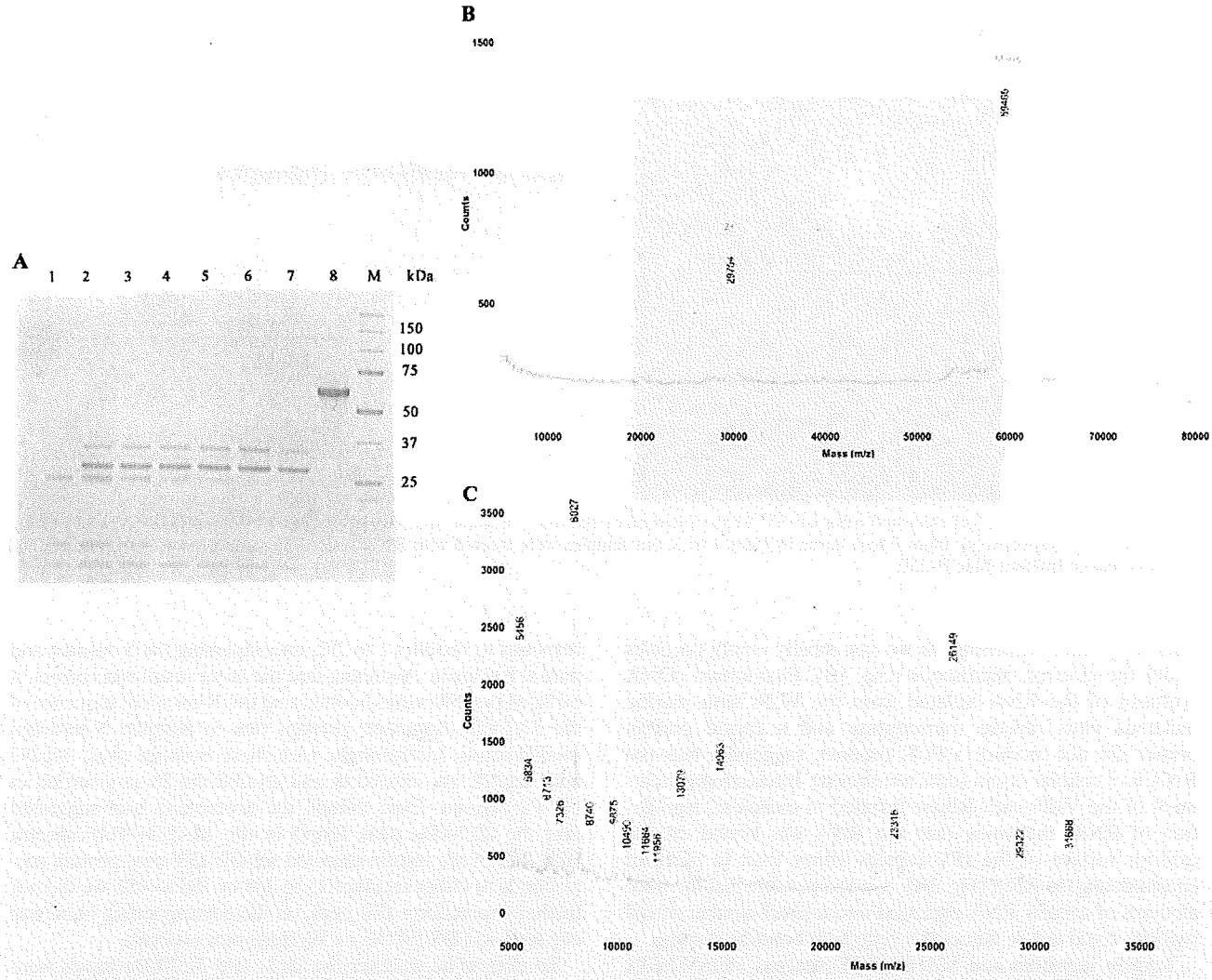

FIG. 4. SDS-PAGE and MALDI-TOF analysis of trypsin- or buffer-treated rSV particles. rSV particles were incubated with decreasing concentrations of trypsin for 30 min at 37°C and then electrophoresed on 4 to 12% bis-Tris gels. Bands were visualized by staining with Simple blue. (A) Lane 1, trypsin alone (250 μg/ml); lanes 2 to 7, rSV incubated with an equal volume of trypsin at 500 μg/ml (lane 2), 250 μg/ml (lane 3), 125 μg/ml (lane 4), 62.5 μg/ml (lane 5), 31.2 μg/ml (lane 6), and 15.6 μg/ml (lane 7); lane 8, buffer-treated rSV particles; lane M, protein molecular mass marker. The arrow indicates the trypsin band. (B and C) MALDI-TOF analysis of buffer-treated (B) and trypsin (62.5 μg/ml)-treated (C) rSV particles.

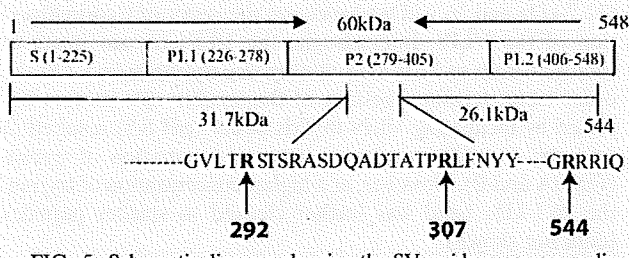

FIG. 5. Schematic diagram showing the SV residues corresponding to different structural domains, trypsin digestion fragments, and the sequence/location of trypsin cleavage sites. The arrows indicate amino acids 292, 307, and 544, where trypsin specific cleavage occurs in the assembled form of the rSV capsids.

amino acids are conserved in the P domain. The capsid protein of SV has 548 amino acid residues, whereas NV CP is composed of 530 amino acids. Alignment of these sequences revealed that the extra 18 aa present in the SV capsid protein resulted in a large insertion in the P2 domain (Fig. 8). Prediction of trypsin cleavage sites in the amino acid sequence of SV coat protein by using a web-based tool (http://ca.expasy.org/tools/peptidecutter/) suggested that there are 35 trypsin cleavage sites in the SV sequence, compared to 25 in the NV capsid protein. Of these 25 sites, only 3 trypsin cleavage sites are present in the P2 domain (aa 278 to 405) of NV, whereas 12 of the 35 potential sites are present in the P2 domain of the SV capsid protein. These 12 trypsin cleavage sites are conserved among all members of GII.3. In addition, the arginine/lysine residue at position 287 (P2 domain) is conserved in all human NoVs sequenced to date (Fig. 8). How-

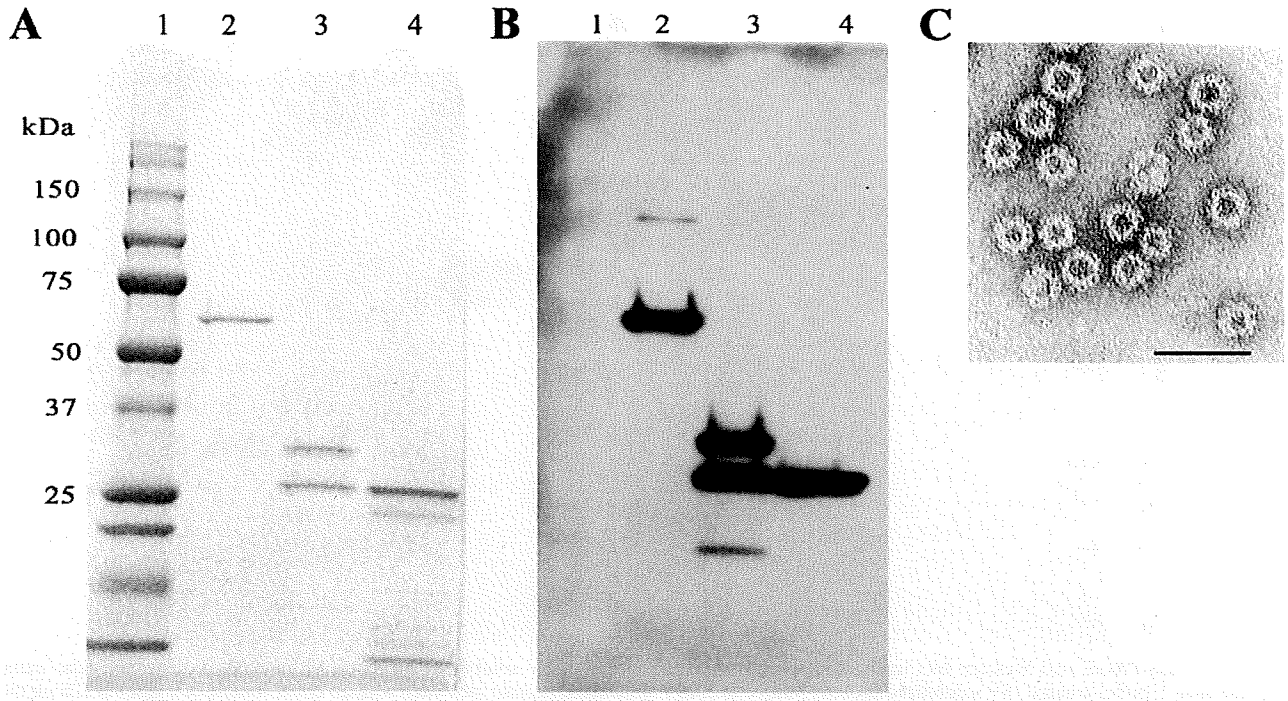

FIG. 6. SDS-PAGE, Western analysis, and electron microscopy characterization of sucrose gradient fractions of buffer-treated and trypsin (62.5 μg/ml)-treated rSV particle. (A) Lane 1, protein molecular mass marker; lane 2, buffer-treated rSV particles; lane 3, trypsin-treated rSV particles obtained from the center of the gradient; lane 4, trypsin-treated rSV protein obtained from the top of the gradient. (B) Western blot of the samples in panel A. (C) Electron micrographs of the trypsin-treated and gradient-purified rSV particles. Bar, 100 nm.

ever, based on the modeling studies, this residue does not appear to be accessible for trypsinization in the assembled form of the coat protein.

Homology modeling of the Sinsiro virus capsid protein and mapping of trypsin cleavage sites. A structural model of Sinsiro virus capsid protein was built using the Norwalk virus capsid protein as the structural template, as described in Materials and Methods section. The resulting model is nearly identical to that of Norwalk virus coat protein, with the exception of a 20-aa insertion (residues 297 to 316) in the P2 domain of the Sinsiro virus coat protein. This insertion forms a surface-exposed loop in the assembled form of the coat protein (Fig. 9). Furthermore, the two trypsin cleavage sites are either part of this loop (Arg307) or four residues upstream of the insertion (Arg292), and these residues are surface accessible, consistent with the results from trypsinization experiments. The third site (Arg544) at the C terminus was also found to be surface exposed. Interestingly, in addition to K227, a conserved trypsin cleavage site in the hinge region of NV, three potential trypsinization sites (K289, R291, and K391) in the P2 domain of NV do not appear to be surface accessible in the assembled (capsid) form of the particles.

DISCUSSION

Expression of rSV capsid protein in insect cells resulted in spontaneous formation of VLPs, which are morphologically similar to other NoV capsids. Examination of the purified VLPs under the transmission electron microscope revealed the presence of empty as well as a few full capsids. However, the ratio of empty to full capsids differed from one preparation to another. Even though the majority of the VLPs appeared to be empty under TEM, ethidium bromide staining of VLPs on native agarose gels indicated that there is RNA associated with the particles. However, RNase treatment of VLPs led to complete dissociation/degradation of the RNA, suggesting that the RNA is bound on the external surface of the VLPs (Fig. 3). This perhaps is made possible by the presence of clusters of positively charged amino acids exposed on the surface (Fig. 9). However, it is also possible that the trace amounts of cellular RNA packaged into a very few full particles could not be detected by ethidium bromide staining. In addition, isolation of RNA associated with the VLPs followed by reverse transcription-PCR analysis showed that the RNA does not contain the viral message, and hence it might be of cellular origin.

The results obtained from in vitro trypsin digestion of the intact VLPs followed by N-terminal sequencing and mass spectrometry analysis suggested that the trypsin cleavage sites are located at amino acid residues Arg292, Arg307, and Arg544. Interestingly, two of these residues (Arg292 and Arg307) are located in and around the large insertion of 20 aa in the P2 domain, while the third site, Arg544, is located near the C terminus. Homology modeling studies clearly indicated that this insertion is unstructured and surface exposed, thus facilitating the ease of trypsinization at these three sites (Fig. 9). There is another conserved basic residue (R296) in this loop, which has potential to be trypsinized. However, further proteolysis at residues R292 and R307 on either side of R296 could release the short peptides of residues 293 to 296 and 297 to

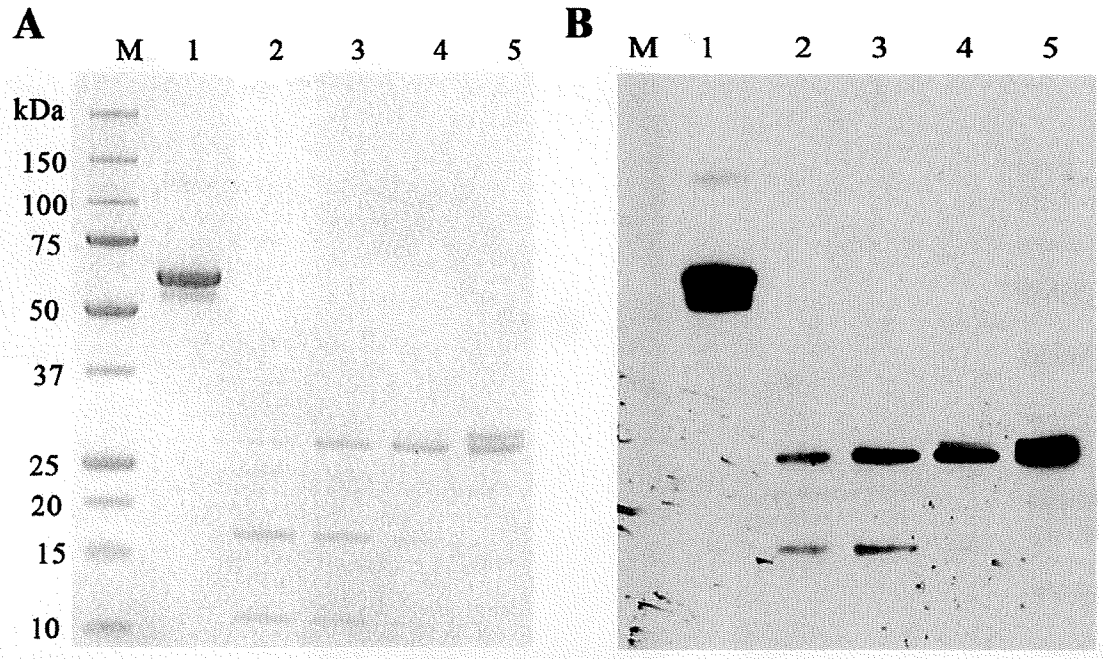

FIG. 7. SDS-PAGE and Western blot analysis of trypsin- and buffer-treated rSV solubilized protein. (A) Lane M, protein molecular mass marker; lane 1, buffer-treated rSV solubilized protein; lanes 2 to 5, rSV solubilized protein incubated with an equal volume of trypsin at 125 μg/ml (lane 2), 62.5 μg/ml (lane 3), 31.2 μg/ml (lane 4), and 15.6 μg/ml (lane 5). (B) Western blot corresponding to the samples in panel A.

306. Hence, the cleavage at residue R296 may not have a significant impact. Remarkably, the large insertion of 20 aa (relative to NV) appears to be a characteristic of the GII.3 and GII.6 NoVs along with the conservation of all three trypsin cleavage sites, implying a potential biological role for this insertion.

Earlier studies by Hardy et al. suggested that NV particles are resistant to trypsinzation (18). They have also shown that the free coat protein subunits undergo trypsinization, thereby releasing the intact P domain. Our results are in good agreement with those of Hardy et al., as the GI.1 NoVs (e.g., Norwalk virus) lack the large surface insertion as seen in the GII.3 viruses (e.g., Sinsiro virus) and none of other basic residues are available for trypsinization in the particle form, except for the cluster of arginines near the C terminus. Hence, the group I NoVs may not undergo trypsinization in the assembled form to release the intact P domain. However, the above results do not support the recent findings reported by Tan et al. (36), who suggested that the NV (GI) and VA387 (GII.4) particles, both of which lack the long insertion (only a 12-aa insertion in the case of VA387) comprised of basic amino acids, undergo partial trypsin digestion, thereby releasing the intact P domains. This is a rather surprising finding, as Lys227 in NV or its counterparts near the hinge regions of other NoVs, which need to be proteolysed to release the P domain, are in fact buried and would be inaccessible for trypsinization in all the intact norovirus capsids. This site would become accessible for trypsinization only in the free and soluble form of the CP

```
Norwalk        (G1_1) 291 RGTSNGTVIN--------------------LTELDG..... SARGRLGLRR 530
Msham-Gbr95    (G2_2) 287 KGEVTAHLHDNDH----------LNNVTITNLNG..... GRRRVQ---- 542
Hilingd-GBR00  (G2_5) 287 RGKVTGQFPNEQN----------MWNLEITNLNG..... GRRRFQ---- 540
Erfurt-DEU01   (G2_10)287 RGKVTQQVQDEHRG---------THWNMTVTNLNG..... GRRRMQ---- 548
Hawaii-USA91   (G2_1) 287 RGRINAQVPDDHH----------QWNLQVTNTNG..... GRRRVQ---- 535
Amstdam-NLD99  (G2_8) 287 RGTLQTR----------LADQPNYTYQVHLENLDG..... GRRRVQ---- 537
VABeach-USA01  (G2_9) 287 KGTLQAE----------VPG-QHQLYQLQLTNLDG..... GRRRIQ---- 537
Leeds-GBR00    (G2_7) 287 KGEVIAK----------NGDVRSYRMDMEITNTDG..... GRRRVQ---- 540
Toronto-CAN93  (G2_3) 287 RGTLTRSTSRASDQADTPTPRLFNYYWHIQLDNLNG..... GRRRIQ---- 548
Sinsiro        (G2_3) 287 RGVLTRSTSRASDQADTATPRLFNYYWHVQLDNLNG..... GRRRIQ---- 548
Seacrof-GBR00  (G2_6) 286 RGTLISQTARAADSTDSPQ-RARNHPLHVQVKNLDG..... GRRRAQ---- 550
Bristol-GBR93  (G2_4) 287 RGDVTHIAG--------------SHDYTMNLASQNW..... GRRRAL---- 539
VA387          (G2_4) 287 RGDVTHIAG--------------SHDYIMNLASQNW..... GRRRAL---- 539
```

FIG. 8. Sequence alignment of the P2 domains of various strains of NoVs belonging to different genogroups, where a large insertion occurs in Sinsiro virus. The boxed sequence represents the 20-amino-acid insertion in the GII.3 and GII.6 NoVs with respect to Norwalk virus (GI.1). The genogroup classification of each strain is shown in parentheses. The start and end residue numbers corresponding to each sequence are listed. Arginine residues that undergo trypsinization in SV are underlined.

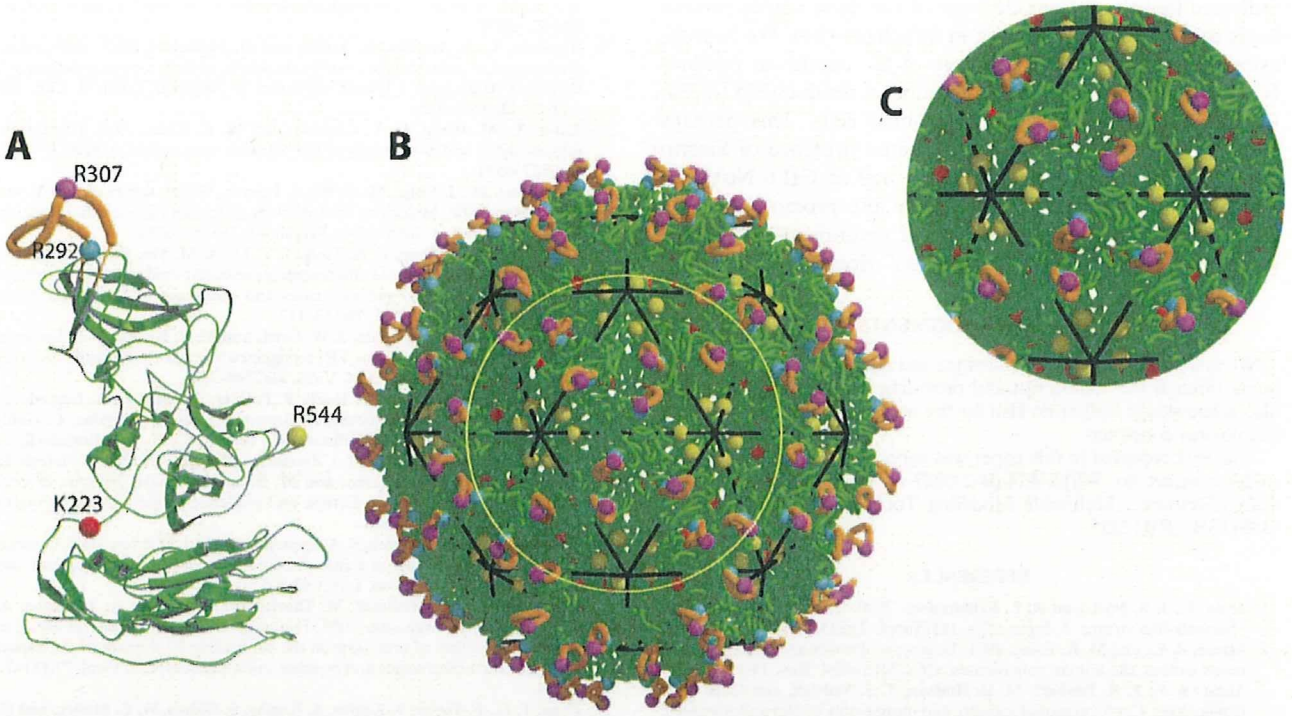

FIG. 9. Comparative model of the SV capsid, generated using NV as the structural model. (A) Ribbon diagram showing the tertiary fold of the SV coat protein subunit (green), which is superimposed on the subunit of Norwalk virus (thin gray tube). The 20-aa insertion is highlighted in orange. Locations of the SV residues that undergo (R292, R307, R544) or have the potential to but did not undergo (K223) trypsin digestion in the particle form are shown as spheres, and the corresponding residue numbers are listed. The residues shown in gray and black spheres are those of the Norwalk virus coat protein which are not accessible for trypsinization in the particle form. (B) A complete capsid model of SV, showing the relative dispositions and exposures of the residues. (C) Zoom-in view of the highlighted (circular) region of the capsid in panel B.

subunits or at minimum in the disassembled and/or partially assembled forms of capsids.

Sinsiro virus has 12 trypsin cleavage sites (Arg287, Arg292, Arg296, Arg307, Arg341, Lys343, Arg351, Arg358, Lys363, Arg370, Lys374, and Arg394) in the P2 domain. Based on the trypsin digestion experiments and modeling studies, the trypsin cleavage sites at Arg292 and Arg307 are accessible to trypsinization even in the assembled VLPs. In contrast, there are only three potential trypsin cleavage sites (Lys289, Arg291, and Lys391) present in the P2 domain of NV. Based on modeling studies, all these sites appeared to be buried, except for residue Lys391, which is partially exposed. However, none of these sites have been reported to be accessible for trypsin digestion in the assembled form of Norwalk virus (18, 36).

Remarkably, TEM characterization of the trypsin-treated rSV particles revealed that the VLPs remain intact even after trypsin digestion (Fig. 6C). The cleaved fragments remain associated with the rest of capsid, perhaps due to close interactions between the P domains up to 72 h after trypsin treatment. Trypsin digestion of the soluble capsid protein of SV obtained by disassembly of VLPs showed a single 26.1-kDa fragment (aa 308 to 544) of the P domain, which is resistant to further proteolysis at low concentrations of trypsin (Fig. 6). This clearly shows that Arg307 is accessible for trypsinization in both the assembled and unassembled forms of the Sinsiro virus coat protein subunits. However, higher concentrations of trypsin led to complete degradation of SV capsid protein (data not shown). We surmise that the 31.7-kDa fragment in its unassembled form is digested into smaller fragments even at low concentrations of trypsin.

Earlier studies suggested that the hypervariable region of the P2 domain (aa 300 to 405) of NV is the main region where immune response-driven mutations are localized (26). In addition, the P2 domain also contains the determinants for strain specificity (29). Moreover, monoclonal antibodies that recognize residues 300 to 384 in the P2 domain readily inhibit the binding of NV capsids to cells (39). Several studies using recombinant peptides and domain swaps have shown that the neutralization epitopes in feline calicivirus also map to the hypervariable region in the P2 domain (37). Recently, Lochridge et al. further narrowed down the antigenic epitopes to amino acids 291 to 293 and 313 to 322 in the P2 domains of NV and Snow Mountain virus, which are the reference strains of GI.1 and GII.2, respectively (23). The linear epitope composed of amino acids 313 to 322 in Snow Mountain virus, which has been suggested to be responsible for the host cell interactions, is conserved among all the NoVs (23). Remarkably, the corresponding residues 325 to 334 in SV remain contiguous even after trypsin digestion, suggesting that the trypsin-treated particles, in principle, are capable of binding to cells.

For viruses that replicate on mucosal surfaces and particularly in the gastrointestinal tract, proteolytic cleavage of outer capsid proteins plays an important role in the replication cycle of the parent viruses. Previous studies on rotaviruses clearly

indicated that the trypsin cleavage of the outer capsid protein leads to a severalfold increase in infectivity (11). We hypothesize that the proteolytic cleavage of SV capsids at residues R292 and R307 results in less restraint on residues 325 to 334, thereby enhancing their ability to bind cells. This perhaps could be one of the reasons for greater virulence of Sinsiro virus and GII.3 NoVs in general, as well as GII.6 NoVs. In addition, the proteolytic cleavage may also promote the viral infection by inhibiting the binding of neutralizing antibodies against the native virus to the "nicked" virus.

ACKNOWLEDGMENTS

We thank Milena Iacobelli-Martinez and Ajay Vashisht for carefully going through the manuscript and providing helpful suggestions. We also acknowledge Catherine Hsu for the help and advice in generating baculovirus constructs.

The work reported in this paper was supported by the USAMRIID under contract no. W81XWH-04-2-0027 to V.S.R. and by NIH Research Resource: Multiscale Modeling Tools for Structural Biology (MMTSB), RR12255.

REFERENCES

1. **Ando, T., J. S. Noel, and R. L. Fankhauser.** 2000. Genetic classification of "Norwalk-like viruses. J. Infect. Dis. **181**(Suppl. 2):S336–S348.
2. **Atmar, R. L., and M. K. Estes.** 2001. Diagnosis of noncultivatable gastroenteritis viruses, the human caliciviruses. Clin. Microbiol. Rev. **14**:15–37.
3. **Ausar, S. F., T. R. Foubert, M. H. Hudson, T. S. Vedvick, and C. R. Middaugh.** 2006. Conformational stability and disassembly of Norwalk virus-like particles. Effect of pH and temperature. J. Biol. Chem. **281**:19478–19488.
4. **Baker, T. S., J. Drak, and M. Bina.** 1988. Reconstruction of the three-dimensional structure of simian virus 40 and visualization of the chromatin core. Proc. Natl. Acad. Sci. USA. **85**:422–426.
5. **Baker, T. S., W. W. Newcomb, N. H. Olson, L. M. Cowsert, C. Olson, and J. C. Brown.** 1991. Structures of bovine and human papillomaviruses. Analysis by cryoelectron microscopy and three-dimensional image reconstruction. Biophys. J. **60**:1445–1456.
6. **Baker, T. S., N. H. Olson, and S. D. Fuller.** 1999. Adding the third dimension to virus life cycles: three-dimensional reconstruction of icosahedral viruses from cryo-electron micrographs. Microbiol. Mol. Biol. Rev. **63**:862–922.
7. **Bertolotti-Ciarlet, A., L. J. White, R. Chen, B. V. Prasad, and M. K. Estes.** 2002. Structural requirements for the assembly of Norwalk virus-like particles. J. Virol. **76**:4044–4055.
8. **Carrascosa, J. L., and A. C. Steven.** 1978. A procedure for evaluaton of significant structural differences between related arrays of protein molecules. Micron **9**:199–206.
9. **Chakravarty, S., A. M. Hutson, M. K. Estes, and B. V. Prasad.** 2005. Evolutionary trace residues in noroviruses: importance in receptor binding, antigenicity, virion assembly, and strain diversity. J. Virol. **79**:554–568.
10. **Chen, R., J. D. Neill, M. K. Estes, and B. V. Prasad.** 2006. X-ray structure of a native calicivirus: structural insights into antigenic diversity and host specificity. Proc. Natl. Acad. Sci. USA. **103**:8048–8053.
11. **Crawford, S. E., S. K. Mukherjee, M. K. Estes, J. A. Lawton, A. L. Shaw, R. F. Ramig, and B. V. Prasad.** 2001. Trypsin cleavage stabilizes the rotavirus VP4 spike. J. Virol. **75**:6052–6061.
12. **Fankhauser, R. L., S. S. Monroe, J. S. Noel, C. D. Humphrey, J. S. Bresee, U. D. Parashar, T. Ando, and R. I. Glass.** 2002. Epidemiologic and molecular trends of"Norwalk-like viruses" associated with outbreaks of gastroenteritis in the United States. J. Infect. Dis. **186**:1–7.
13. **Fankhauser, R. L., J. S. Noel, S. S. Monroe, T. Ando, and R. I. Glass.** 1998. Molecular epidemiology of "Norwalk-like viruses" in outbreaks of gastroenteritis in the United States. J. Infect. Dis. **178**:1571–1578.
14. **Gallimore, C. I., D. Lewis, C. Taylor, A. Cant, A. Gennery, and J. J. Gray.** 2004. Chronic excretion of a norovirus in a child with cartilage hair hypoplasia (CHH). J. Clin. Virol. **30**:196–204.
15. **Glass, P. J., L. J. White, J. M. Ball, I. Leparc-Goffart, M. E. Hardy, and M. K. Estes.** 2000. Norwalk virus open reading frame 3 encodes a minor structural protein. J. Virol. **74**:6581–6591.
16. **Green, K. Y., A. Z. Kapikian, J. Valdesuso, S. Sosnovtsev, J. J. Treanor, and J. F. Lew.** 1997. Expression and self-assembly of recombinant capsid protein from the antigenically distinct Hawaii human calicivirus. J. Clin. Microbiol. **35**:1909–1914.
17. **Green, S. M., P. R. Lambden, E. O. Caul, and I. N. Clarke.** 1997. Capsid sequence diversity in small round structured viruses from recent UK outbreaks of gastroenteritis. J. Med. Virol. **52**:14–19.
18. **Hardy, M. E., L. J. White, J. M. Ball, and M. K. Estes.** 1995. Specific proteolytic cleavage of recombinant Norwalk virus capsid protein. J. Virol. **69**:1693–1698.
19. **Hirakata, Y., K. Arisawa, O. Nishio, and O. Nakagomi.** 2005. Multiprefectural spread of gastroenteritis outbreaks attributable to a single genogroup II norovirus strain from a tourist restaurant in Nagasaki, Japan. J. Clin. Microbiol. **43**:1093–1098.
20. **Jiang, X., M. Wang, D. Y. Graham, and M. K. Estes.** 1992. Expression, self-assembly, and antigenicity of the Norwalk virus capsid protein. J. Virol. **66**:6527–6532.
21. **Koopmans, M., J. Vinje, M. de Wit, I. Leenen, W. van der Poel, and Y. van Duynhoven.** 2000. Molecular epidemiology of human enteric caliciviruses in The Netherlands. J. Infect. Dis. **181**(Suppl. 2):S262–S269.
22. **Lau, C. S., D. A. Wong, L. K. Tong, J. Y. Lo, A. M. Ma, P. K. Cheng, and W. W. Lim.** 2004. High rate and changing molecular epidemiology pattern of norovirus infections in sporadic cases and outbreaks of gastroenteritis in Hong Kong. J. Med. Virol. **73**:113–117.
23. **Lochridge, V. P., K. L. Jutila, J. W. Graff, and M. E. Hardy.** 2005. Epitopes in the P2 domain of norovirus VP1 recognized by monoclonal antibodies that block cell interactions. J. Gen. Virol. **86**:2799–2806.
24. **Lopman, B., H. Vennema, E. Kohli, P. Pothier, A. Sanchez, A. Negredo, J. Buesa, E. Schreier, M. Reacher, D. Brown, J. Gray, M. Iturriza, C. Gallimore, B. Bottiger, K. O. Hedlund, M. Torven, C. H. von Bonsdorff, L. Maunula, M. Poljsak-Prijatelj, J. Zimsek, G. Reuter, G. Szucs, B. Melegh, L. Svennson, Y. van Duijnhoven, and M. Koopmans.** 2004. Increase in viral gastroenteritis outbreaks in Europe and epidemic spread of new norovirus variant. Lancet **363**:682–688.
25. **Meakins, S. M., G. K. Adak, B. A. Lopman, and S. J. O'Brien.** 2003. General outbreaks of infectious intestinal disease (IID) in hospitals, England and Wales, 1992–2000. J. Hosp. Infect **53**:1–5.
26. **Nilsson, M., K. O. Hedlund, M. Thorhagen, G. Larson, K. Johansen, A. Ekspong, and L. Svensson.** 2003. Evolution of human calicivirus RNA in vivo: accumulation of mutations in the protruding P2 domain of the capsid leads to structural changes and possibly a new phenotype. J. Virol. **77**:13117–13124.
27. **Phan, T. G., F. Yagyu, V. Kozlov, A. Kozlov, S. Okitsu, W. E. Muller, and H. Ushijima.** 2006. Viral gastroenteritis and genetic characterization of recombinant norovirus circulating in Eastern Russia. Clin. Lab. **52**:247–253.
28. **Pletneva, M. A., S. V. Sosnovtsev, and K. Y. Green.** 2001. The genome of Hawaii virus and its relationship with other members of the caliciviridae. Virus Genes **23**:5–16.
29. **Prasad, B. V., M. E. Hardy, T. Dokland, J. Bella, M. G. Rossmann, and M. K. Estes.** 1999. X-ray crystallographic structure of the Norwalk virus capsid. Science **286**:287–290.
30. **Reuter, G., H. Vennema, M. Koopmans, and G. Szucs.** 2006. Epidemic spread of recombinant noroviruses with four capsid types in Hungary. J. Clin. Virol. **35**:84–88.
31. **Rohayem, J., J. Munch, and A. Rethwilm.** 2005. Evidence of recombination in the norovirus capsid gene. J. Virol. **79**:4977–4990.
32. **Sali, A., and T. L. Blundell.** 1993. Comparative protein modelling by satisfaction of spatial restraints. J. Mol. Biol. **234**:779–815.
33. **Schneemann, A., R. Dasgupta, J. E. Johnson, and R. R. Rueckert.** 1993. Use of recombinant baculoviruses in synthesis of morphologically distinct virus-like particles of flock house virus, a nodavirus. J. Virol. **67**:2756–2763.
34. **Shepherd, C. M., I. A. Borelli, G. Lander, P. Natarajan, V. Siddavanahalli, C. Bajaj, J. E. Johnson, C. L. Brooks III, and V. S. Reddy.** 2006. VIPERdb: a relational database for structural virology. Nucleic Acids Res. **34**:D386–D389.
35. **Tan, M., P. Huang, J. Meller, W. Zhong, T. Farkas, and X. Jiang.** 2003. Mutations within the P2 domain of norovirus capsid affect binding to human histo-blood group antigens: evidence for a binding pocket. J. Virol. **77**:12562–12571.
36. **Tan, M., J. Meller, and X. Jiang.** 2006. C-terminal arginine cluster is essential for receptor binding of norovirus capsid protein. J. Virol. **80**:7322–7331.
37. **Tohya, Y., N. Yokoyama, K. Maeda, Y. Kawaguchi, and T. Mikami.** 1997. Mapping of antigenic sites involved in neutralization on the capsid protein of feline calicivirus. J. Gen. Virol. **78**:303–305.
38. **Vinje, J., J. Green, D. C. Lewis, C. I. Gallimore, D. W. Brown, and M. P. Koopmans.** 2000. Genetic polymorphism across regions of the three open reading frames of "Norwalk-like viruses." Arch. Virol. **145**:223–241.
39. **White, L. J., J. M. Ball, M. E. Hardy, T. N. Tanaka, N. Kitamoto, and M. K. Estes.** 1996. Attachment and entry of recombinant Norwalk virus capsids to cultured human and animal cell lines. J. Virol. **70**:6589–6597.
40. **White, L. J., M. E. Hardy, and M. K. Estes.** 1997. Biochemical characterization of a smaller form of recombinant Norwalk virus capsids assembled in insect cells. J. Virol. **71**:8066–8072.
41. **Zheng, D. P., T. Ando, R. L. Fankhauser, R. S. Beard, R. I. Glass, and S. S. Monroe.** 2006. Norovirus classification and proposed strain nomenclature. Virology **346**:312–323.
42. **Zintz, C., K. Bok, E. Parada, M. Barnes-Eley, T. Berke, M. A. Staat, P. Azimi, X. Jiang, and D. O. Matson.** 2005. Prevalence and genetic characterization of caliciviruses among children hospitalized for acute gastroenteritis in the United States. Infect. Genet. Evol. **5**:281–290.

Microbiology and Immunology

Microbiol Immunol 2009; **53**: 356–359
doi:10.1111/j.1348-0421.2009.00132.x

NOTE

Seroepidemiological study of norovirus infection in Aichi Prefecture, Japan

Shinichi Kobayashi[1], Noriko Fujiwara[1], Naokazu Takeda[2] and Hiroko Minagawa[1]

[1]Laboratory of Virology, Department of Microbiology and Medical Zoology, Aichi Prefectural Institute of Public Health, 7-6 Nagare, Tsujimachi, Kita-ku, Nagoya 462-8576 and [2]Department of Virology II, National Institute of Infectious Diseases, 4-7-1 Gakuen, Musashimurayama, Tokyo 208-0011, Japan

ABSTRACT

The serological prevalence of IgG antibody to seven NoV strains (GI.1, GI.4, GII.3, GII.4, GII.10, GII.12 and GII.15) among inhabitants aged 1–62 years of Aichi Prefecture, Japan was studied. Age-related seroprevalence was measured by ELISA using baculovirus-expressed recombinant VLP antigens. Seropositive rates for all seven VLP antigens gradually increased with age. Among the tested antigens, the highest seropositive rate was for the GII.4 strain. This result is consistent with the recent epidemic of NoV infection due to GII.4 strain in Japan.

Key words norovirus, seroepidemiology, virus-like particles

NoV, a genus in the *Caliciviridae* family, is a major cause of both sporadic cases and large outbreaks of acute non-bacterial gastroenteritis in people of all ages worldwide (1–3). NoV infection spreads very rapidly by person-to-person transmission, aerosol transmission of vomit and contaminated food or water (3).

NoV strains can be classified into five genogroups (GI to GV) based on genetic diversity (4). Major human NoV strains belong to GI and GII, which can be further subdivided into at least 14 and 17 genotypes (GI.1 to GI.14 and GII.1 to GII.17), respectively (5, 6).

Large-scale seroepidemiological studies have been restricted due to inability to propagate NoV by cell culture. Early serological studies relied on clinical samples of viral antigens derived from infected volunteers or patients with gastroenteritis (7, 8). Later successful expression of the capsid protein of the prototype Norwalk virus in a baculovirus expression system enabled researchers to obtain an abundant supply of antigens for epidemiological studies (9, 10). The expressed capsid proteins were found to form VLP which are morphologically and antigenically similar to native NV (11).

In this study, we used ELISA based on baculovirus-expressed VLP antigens to examine the prevalence of antibodies to seven NoV strains among inhabitants of Aichi Prefecture, Japan. We previously expressed five NoV strains including GI.1 (SeV strain, AB031013), GI.4 (CV strain, AB042808), GII.3 (Sinsiro strain, AB195226), GII.4 (Narita strain, AB078336 and GII.12 (Chitta strain, AB032758) (12). In this study, we expressed two additional VLP from the Hokushin and Kamo strains by using a baculovirus expression system as previously described (13). The Hokushin strain, associated with a food-borne outbreak in Nagano Prefecture, Japan, in 2003, and the Kamo strain, derived from a food-borne outbreak in Aichi Prefecture in 2003, were genotyped as GII.10 and GII.15,

Correspondence
Shinichi Kobayashi, Laboratory of Virology, Aichi Prefectural Institute of Public Health, 7-6 Nagare, Tsujimachi, Kita-ku, Nagoya 462-8576, Japan. Tel: +81 52 910 5674; fax: +81 52 913 3641; email: shinichi_kobayashi@pref.aichi.lg.jp

Received 23 December 2008; revised 11 February 2009; accepted 16 February 2009.

List of Abbreviations: aa, amino acid; BSA, bovine serum albumin; 1% BSA-PBS, PBS containing 1% BSA; ELISA, enzyme-linked immunosorbent assay; GI, genogroup I; GII, genogroup II; HRP, horseradish peroxidase, IgG, immunoglobulin G; I LV, Lordsdale virus; MxV, Mexico virus; NV, Norwalk virus; NoV, norovirus; ORF, open reading frame; PBS, phosphate buffered saline; PBS-T, 0.01 M phosphate buffered saline (pH 7.4) containing 0.1% Tween 20; RT-PCR, reverse transcription-polymerase chain reaction; SeV, Seto virus; SV, Southampton virus; TMB, tetramethylbenzidine, VLP, virus-like particles.

Table 1 Percentage identities between each pair of entire ORF2 nucleotide sequences (upper right triangle) and deduced amino acid sequences (lower left triangle) of NoV strains

Genogroup			GI		GII				
	Genotype		1	4	3	4	10	12	15
		Strains	SeV	CV	Sinsiro	Narita	Hokusin	Chitta	Kamo
GI	1	SeV	*	65.9	52.0	50.9	51.1	54.4	52.5
	4	CV	72.1	*	52.0	52.9	54.7	54.0	53.7
GII	3	Sinsiro	45.0	43.5	*	64.9	65.6	66.9	66.9
	4	Narita	43.5	43.8	65.7	*	63.9	64.3	65.8
	10	Hokushin	47.3	43.3	67.2	62.8	*	64.7	70.0
	12	Chitta	45.9	44.7	70.0	64.9	77.2	*	74.1
	15	Kamo	46.4	45.7	69.0	65.4	75.0	79.4	*

respectively (5). The entire capsid genes of the Hokushin and Kamo strains were amplified by RT-PCR using G2Fb and G2R04 primers (12). Nucleotide sequence analysis indicated that the ORF2 genes of the Hokushin (AB195227) and Kamo (AB195228) strains are predicted to consist of 1647 nucleotides (549 aa) and 1623 nucleotides (541 aa), respectively. The nucleotide and aa sequences of the entire open reading frame (ORF) 2 genes of seven NoV strains used in this study are compared in Table 1. The Hokushin strain has 62.8–77.2% nucleotides (63.9–70.0% aa) identity with other GII NoV and 43.3–47.3% nucleotides (51.1–54.7% aa) identity with GI NoV. The Kamo strain showed 65.4–79.4% nucleotides (65.8–74.1% aa) identity with GII NoV and 45.7–46.4% nucleotides (52.5–53.7% aa) identity with GI NoV. Recombinant capsid proteins of the Hokushin and Kamo strains were expressed in insect cells, and then VLP formation was confirmed by electron microscopy as described previously (13).

Antigen capture ELISA using polyclonal antisera to seven recombinant capsid proteins was used to examine the antigenic relationship among seven VLP. The capture ELISA strongly reacted with the homologous VLP. The sensitivity of the assay was approximately 0.01 ng VLP/well, but the assay was unable to detect heterologous VLP at concentrations up to 10 ng/well. Two newly expressed VLP were confirmed to be antigenically differentiated from five previously characterized VLP.

After obtaining informed consent from each individual or his/her parent in the case of minors, a total of 400 serum samples was obtained from infants and children (aged 1 to 17 years) who attended sentinel hospitals, and from healthy adults (aged 18 to 62 years) in Aichi Prefecture, Japan. All samples were collected as part of a seroepidemiological survey based on the National Epidemiological Surveillance of Vaccine-preventable Diseases program in Japan during the period from July to September in 2006 and 2007.The obtained 400 serum samples (200 for each year) were separated into 10 age groups, and the sera were tested for IgG antibody to seven VLP derived from SeV (GI.1), CV (GI.4), Sinsiro (GII.3), Narita (GII.4), Hokushin (GII.10), Chitta (GII.12) and Kamo (GII.15) using ELISA.

The wells of 96 flat-bottomed microtiter plates (Nunc Immuno Maxisorp, Thermo Fisher Scientific, Tokyo, Japan) were each coated with 100 μl of one of the seven VLP (1 μg/ml in 0.05 M carbonate buffer, pH 9.6) and left overnight at 4°C. For a negative control, plates were coated with carbonate buffer alone to detect nonspecific binding. The wells were washed three times with PBS-T and then blocked with 200 μl of PBS containing 2% BSA overnight at 4°C. After washing four times with PBS-T, 100 μl of serum samples diluted to 1:1000 in 1% BSA-PBS was added, and the plates were incubated for 1 hr at 37°C. The wells were washed four times with PBS-T, and then 100 μl of HRP-conjugated goat anti-human IgG (H+L) (Zymed, San Francisco, CA, USA) diluted to 1:5000 in 1% BSA-PBS was added to each well. The plates were incubated for 1 hr at 37°C. The wells were washed five times with PBS-T, and then 100 μl of TMB peroxidase substrate solution (Moss, Pasadena, Maryland, USA) was added to each well. The plates were left for 10 min at room temperature, and then the reaction was stopped with 50 μl of 2 M H_2SO_4. Absorbance at 450 nm was read by a microtiter plate reader Model 690 (Bio-Rad, Hercules, CA, USA). The cutoff point of the test (absorbance at 450 nm > 0.15) was established as the mean of the absorbance at 450 nm of the negative control wells plus three standard deviations.

The age-related prevalence of IgG antibody in seven VLP among inhabitants of Aichi Prefecture, Japan, is shown in Figure 1. Seropositive rates gradually increased with age from 5–30% in the 0–2 year age-group to 45–95% in the 50–62 year age-group in 2006, and from 0–25% in the 0–2 year age-group to 50–90% in the 50–62 year